

14 aug. 1961

TRAINING CENTER FOR EXPERIMENTAL AERODYNAMICS

LEADING EDGE EFFECT

ON SEPARATED SUPERSONIC FLOWS

BY

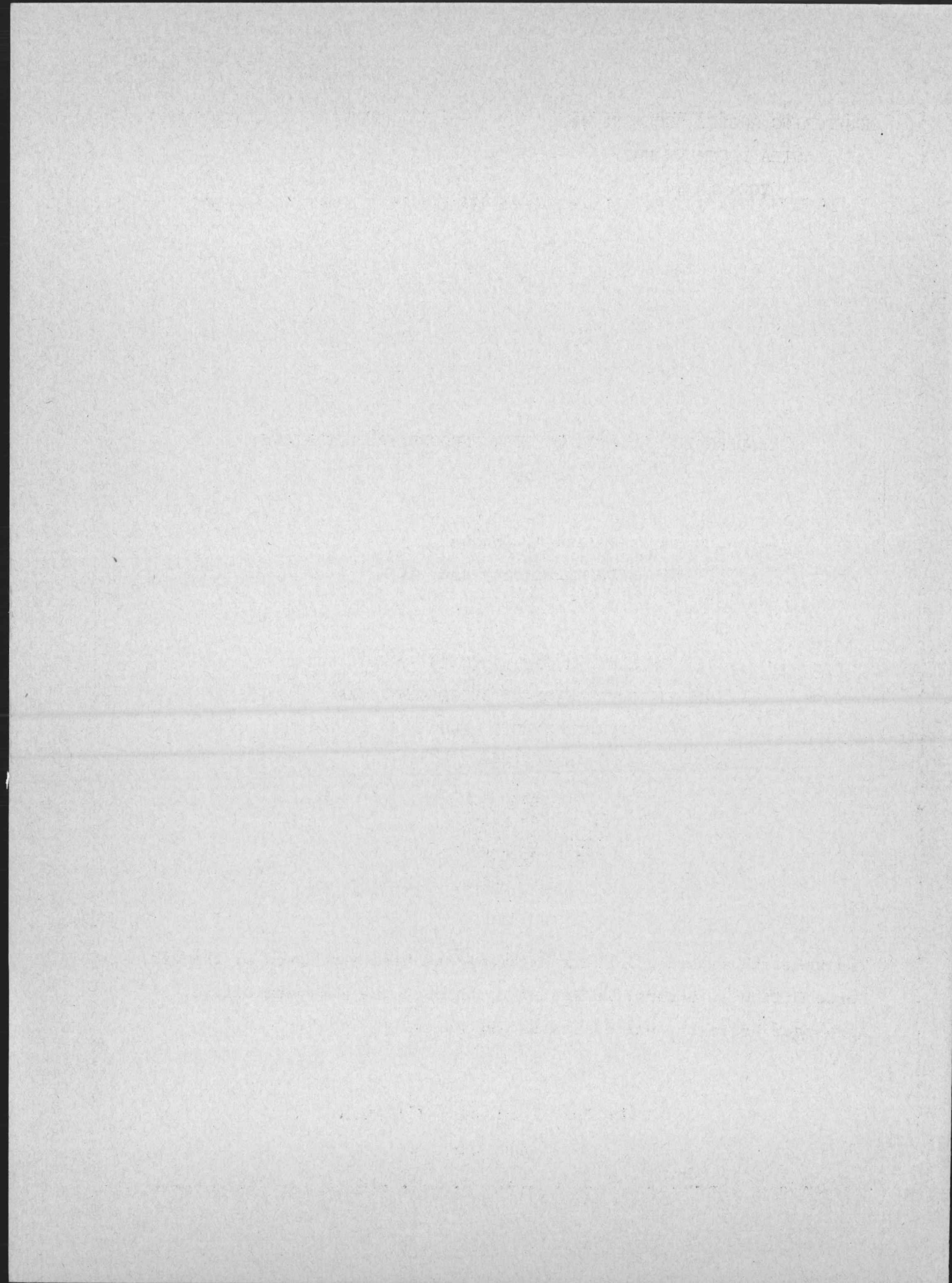
J. J. GINOUX



Rhode - Saint - Genèse, Belgium.

MAY 1961

TCEA TN4



MONITORING AGENCY DOCUMENT NR.

ASTIA DOCUMENT NR.

TCEA TN 4

LEADING EDGE EFFECT ON SEPARATED SUPERSONIC FLOWS

by

Jean J. Ginoux

Brussels University and TCEA

CONTRACT NR. AF 61 (052) - 350

LAMINAR SEPARATION IN SUPERSONIC FLOW

TECHNICAL NOTE NR. 1

May 1961

The research reported in this document has been sponsored by the Air Force Office of Scientific Research, through the European Office, Aerospace Research, United States Air Force.

RESEARCH REPORT ON THE HISTORY OF THE

RESEARCH REPORT ON THE HISTORY OF THE

RESEARCH REPORT ON THE HISTORY OF THE

RESEARCH REPORT ON THE HISTORY OF THE

RESEARCH REPORT ON THE HISTORY OF THE

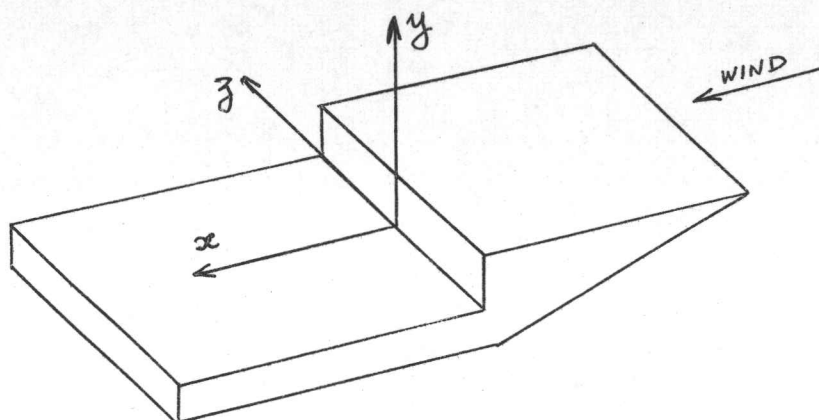
RESEARCH REPORT ON THE HISTORY OF THE

FOREWORD

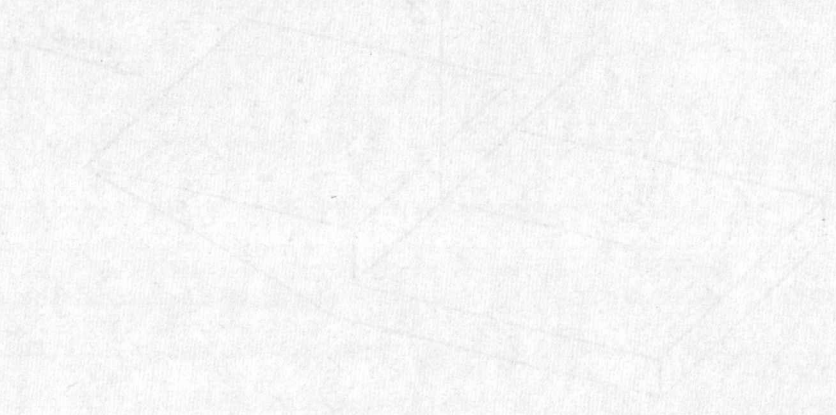
The author would like to thank the European Office of the Office of Aerospace Research (EOAR) for the sponsorship of this work and also to record his thanks to CNERA, without whose support this programme of research would not have been started, and from which the author has received every possible help and encouragement.

NOTATION

- x distance along the center-line of the model from the step base; $x > 0$ downstream of the step and $x < 0$ upstream of the step
- y distance perpendicular to the surface of the model (from the probe-axis)
- z span-wise axis, positive as indicated in the figure



- δ boundary-layer thickness
- λ wave-length of the flow perturbations
- p_0 stagnation pressure
- p static pressure
- p_p pitot-pressure
- Δp_p span-wise pitot-pressure variation expressed as a fraction of the pitot-pressure measured on the center-line of the model
- $\Delta p_p'$ difference in Δp_p between a pressure peak and its neighbouring pressure valley
- h step-height
- S model span
- L length of the plate upstream of the step
- ϵ_m mean leading-edge thickness
- $\Delta \epsilon$ maximum local variation of the leading-edge thickness (i.e. maximum difference between neighbouring peaks and troughs)
- B symbol to denote the side-plates of the model



SUMMARY

Following earlier tests (Ref. 1), in the T.C.E.A. supersonic tunnel S-1 (Ref. 2), on a two-dimensional backward-facing step model in which span-wise perturbations were found in the reattachment region, further studies have been made using the same and other similar models. In these later studies, the same three-dimensional perturbations were detected, into the full thickness of the boundary-layer, after reattachment, both in turbulent and laminar regions of the flow. Their amplitude was a maximum in the transition region.

Using a model with a much improved accuracy of manufacture, notably at the leading-edge, it was found that the amplitude of the perturbations was greatly reduced, roughly in proportion to the size of the irregularities of manufacture of the leading-edge itself. As it is unreasonable to expect these to be anything other than random in character, it is concluded that the phenomenon is essentially one of instability in the two-dimensional flow, the main triggering action arising, at least in the earlier tests, from small irregularities in the leading-edge.

INTRODUCTION

In the course of a research programme undertaken at T.C.E.A. on laminar separated supersonic flow, the author found that three-dimensional perturbations existed in the reattachment region of the flow over backward-facing steps (Ref. 1). The periodical span-wise distribution of these perturbations could not be explained by irregularities either in the air-flow upstream of the models or in the models themselves. Surveys made with total-head probes moved in contact with the model surface showed that,

at a Mach number of 2.16, the ratio of the wave-length of the flow perturbations to boundary-layer thickness was a function of the ratio of step-height to boundary-layer thickness, independent upon the span of the model.

In a continuation of the work, span-wise surveys were made at various heights in the boundary-layer in the reattachment region of the flow as well as upstream of the step, in the separated shear-layer and in the transition region. More attention was given to the amplitude of the span-wise pressure variations. The study was completed by a detailed analysis of the influence of leading-edge irregularities on the intensity of the flow perturbations.

DESCRIPTION OF EQUIPMENT

Wind Tunnel

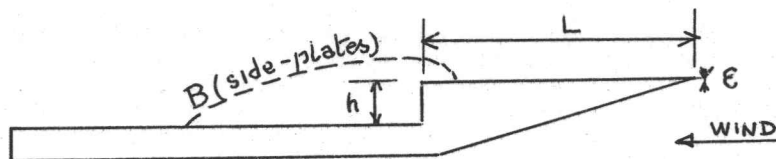
The tests were made in the T.C.E.A. 40 x 40 cm² (16" x 16") continuous supersonic wind tunnel S-1 at a Mach number of about 2.16. A description of the tunnel is given in reference 2.

Model configuration

Several backward facing step models were used in the present investigation. They are shown in Table I, where h is the step-height, L the length of the plate upstream of the step, S the model span, given in millimetres; ϵ_m is the mean leading-edge thickness in microns (i.e. 10^{-3} mm) and $\Delta\epsilon$ the local variations of the thickness (in microns). Models S-20, having a span equal to 200 mm could be fitted with end-plates denoted by the symbol B. Models S-6 and S-20, which did not span the 400 mm test section, were mounted symmetrically in the center of the test section.

Table I

Model configuration and designation



Model	L (mm)	h (mm)	Span, S (mm)	ϵ_m (microns)	$\Delta\epsilon_{\max}$ (microns)
S-3	225	10	400	72	10
S-6	60	3	150	13	7
S-20-c-(B)	80	6	200	224	3
S-20-e-(B)	80	7	200	165	20
S-20-f-(B)	80	7	200	96	3

Surveying mechanism

A sting-support rig, allowing for displacement of probes in three directions was incorporated in the diffuser. It consisted of an axial tube (1.1 m long) supported by two vertical screws (having a 2 mm pitch), the axes of which passed through the upper wall of the tunnel. Their motion was controlled by reversible electric motors, the revolutions being recorded on counters (one revolution of both counters corresponded to a probe displacement of 0.054 mm). Both screws could be rotated independently to allow a vertical translation of the sting as well as a rotation about the center of the test section (± 7 degrees). The sting could slide inside the axial tube; this longitudinal motion was controlled by a reversible electric motor, located in the air-stream at the back-end of the tube, and having a total range of displacement of 50 cm, one revolution of the counter corresponding

to a 1/20 mm displacement of the sting. In addition, the test section could be traversed horizontally along a 150 mm length by fixing a special head to the sting. This consisted of a horizontal slotted wedge having a 180 mm span in which a carriage could slide. The motion was controlled from outside the tunnel by a flexible drive fitted with a revolution counter. The support of the probe was swept forward and fastened to the lower surface of the carriage in such a manner that the nose of the probe was located upstream of the leading-edge of the wedge. The wedge was adjusted in such a way that the nose of the probe could be moved parallel to the model surface during the span-wise surveys.

Test techniques

Transition from laminar to turbulent flow was detected on shadowgraphs and schlieren pictures, taken with a conventional optical system, using parabolic mirrors and a spark light-source.

The flow on the surface of the models was qualitatively observed by the use of a sublimation technique. The indicator chosen was azobenzene, which having a slow response, allowed for the relatively long starting and stopping times of the wind-tunnel. An indication of the surface-flow pattern was generally obtained after 3 to 6 hours running time (depending upon the thickness of the azobenzene layer and the tunnel pressure).

The boundary-layer was surveyed, at different locations (x) from the step, in the span-wise direction (z) and vertically (y), with total head probes of various sizes, fixed to the surveying mechanism already described. The pressure was measured by a differential pressure pick-up and a Brown recorder.

Static pressure distributions were measured along the center line of the models with a multitube manometer using silicone oil.

The leading-edge of the models was examined with a microscope. Each model was mounted vertically on a machine-tool table with its leading-

edge horizontal. A microscope with a magnification of 150 or 300 was translated so as to cover its span. Under the microscope, the leading-edge appeared as a thick band whose coordinates were taken at increments of 0.1 mm over a portion of the span. The accuracy of the measurements was about 1 to 2 microns, depending upon the magnification.

DETAILED SURVEY OF THE BOUNDARY-LAYER FLOW ON MODEL S-3

A detailed survey of the boundary-layer flow was made at a Mach number of 2.16 and at a stagnation pressure of 170 mm of mercury absolute on model S-3 (table I) which had a 10 mm step-height and a flat plate length of 225 mm upstream of the step. The model completely spanned the working section of the wind-tunnel. Using the surveying mechanism, transverse pitot-pressure profiles were recorded at different heights in the boundary-layer and at several distances from the step base; only a portion of the span was surveyed (from $z = 0$ to $z = 60$ mm, except in the separated layer where $0 < z < 40$ mm).

The span-wise pressure variations are expressed as a fraction of pitot-pressure measured on the center-line of the model ($z = 0$) using the following relationship

$$\Delta p_p = \frac{p_p(x, y, z) - p_p(x, y, 0)}{p_p(x, y, 0)}$$

the axes x, y, z being defined as shown under "NOTATION". The results of vertical surveys made at $z = 0$ for different values of x are shown in figure 1, they were used to define the reference pressure $p_p(x, y, 0)$, as well as the boundary-layer thickness (δ). The static pressure distribution along the center-line of the model is given in figure 2.

The results of span-wise surveys are shown in the various graphs of figure 3. The measurements made downstream of reattachment (i.e. for x larger than about 70 mm) indicate that the flow perturbations, previously

detected in the vicinity of the model surface (Ref. 1) extend into the full thickness of the boundary-layer with a maximum variation of pitot-pressure occurring at about mid-thickness, the perturbations in pressure vanishing as the outer edge of the boundary-layer is reached. In the surveys made at $x = 81$ mm, two different cylinder probes were used, having inside diameters of 1.5 mm and 0.25 mm and outside diameters of 2 mm and 0.3 mm respectively; similar results were obtained for both probes as shown in figures 3-9 and 3-10.

The fact that periodical transverse total-head variations were found at various heights in the boundary-layer was an indication that the boundary-layer profile (pressure against height) was periodically distorted along the span of the model. This was confirmed by direct measurement of these profiles at different values of z . The measurements were made at $x = 81$ mm in a region (for $30 < z < 40$ mm, with increments $\Delta z = 1$ mm) where the largest pressure variation was measured in the z -direction. The results are given in figure 4 where the pitot reading, in millimetre of mercury, is plotted against y ; no attempt was made to reduce these data to velocity profiles, as it was possible to measure the wall static pressure only on the center-line of the model. There was therefore no evidence that the static pressure could be taken as constant along the z -direction. From these results, it was possible to evaluate the boundary-layer thickness as a function of z ; as expected, it was found to vary periodically; as seen in figure 4. Similar results were recently obtained at low speed by Schubauer (unpublished).

Surveys were made in the separated boundary-layer at $x = 16$ mm, $x = 45.2$ mm and $x = 63.2$ mm. The nose of the probe was bent in order to be aligned with the flow direction (see figure 5a). The results shown in figure (3-11) indicate that the flow perturbations were mainly localized in the inner portion of the shear-layer (i.e. for y less than about $\delta / 2$).

Measurements made upstream of the step at $x = -5$ mm, -55 mm and -105 mm (figures 3-6 to 3-8) also showed the existence of three-dimensional

perturbations. The variation of pitot-pressure had its maximum value at about mid-thickness and vanished near the outer edge of the boundary-layer. They also vanished near the model surface, which explains why they were never clearly detected in the early part of the research (Ref. 1), either by a probe which was moved in contact with the model surface or by the sublimation technique.

Figures 6a-b give a summary of the results. For each x , one value of y/δ for which the amplitude of the pressure variations was maximum was selected among the available data of figure 3. These values of y/δ are indicated in the upper part of the figure which represents a cross-section of the model (plane x - y) and the corresponding span-wise pressure variations are shown in the lower part of the figure which gives Δp_p (in %) as a function of z (for $0 < z < 60$ mm, except in the free layer for $0 < z < 40$ mm)

These figures show that three-dimensional perturbations existed upstream of separation ($x < 0$) although they were rather weak; a maximum variation $\Delta' p_p$ of about 6 % was found between a pressure peak and its neighbouring pressure valley. As the boundary-layer separated and reattached, the perturbations were progressively amplified to reach a maximum amplitude in the transition region ($\Delta' p_p = 44$ %). They were then extending in the turbulent region of the flow, being slowly damped ($\Delta' p_p = 8$ % at $x = 164.5$ mm). It will be noted that the perturbations were not indicated in that region by the sublimation technique (Ref. 1).

A close observation of figures 5 (with the help of figure 3 where large Δp_p scales are used) shows that the z -position of the peaks and valleys did not vary with x . This is quite clear after separation but not so clear upstream of separation because of the very small amplitudes of most of the perturbations. On the other hand, the repeatability of the measurements was not as good for $x < 0$ as for $x > 0$ and some of the small pressure peaks were not well defined; this is shown in figure 3-12 where different probes were used.

It appears from these results that weak perturbations existed in the boundary-layer before separation, but their amplitude is much greater, they follow a much more regular pattern and in detail they are more repeatable after reattachment.

In reference 3, Hopkins presents photographs of various models coated with fluorescent oil which show evidence of surface vortices at a Mach number of about 3. Some photographs are also presented for the models coated with a sublimation material as was used in the present research. They show that the flow perturbations are more clearly indicated by the fluorescent oil. In particular the "vortices" are visible at a small distance behind the leading edge (i.e. upstream of separation) and it is observed that their spacing increases with the distance from the leading-edge, which is in agreement with Görtler's theory (Ref. 4) derived in the low speed case. The boundary-layer surveys made in the present work did not reveal such a variation of the spacing of the perturbations; it is possible that the probe was not sensitive enough to detect the smallest perturbations.

LEADING-EDGE EFFECT

Evidence was given from the results of the detailed surveys made on model S-3 that the regular pattern of three-dimensional perturbations that existed at reattachment was triggered by the weak perturbations observed in the boundary-layer upstream of separation. The problem was then to find a reason for the existence of these perturbations. In the early part of the research (Ref. 1) it was found that irregularities in the leading-edge of the model could not explain a regular pattern of perturbations. However, not much attention was given at that time to the intensity of the perturbations and it was therefore decided to re-examine the leading-edge effect more carefully. In a series of preliminary tests, several models were tested with accidental or wilful damage in the leading-edge which indicated a strong modification of the intensity of the perturbations. These results finally led to a more systematic investigation during which the effect of the machining accuracy of the leading-edge was examined.

Preliminary Tests

Figure 7a is related to a boundary-layer survey made at $x = -155$ mm (i.e. 70 mm downstream of the leading-edge) on model S-3, in the presence of an accidental notch in the leading-edge, whose approximate size is indicated. It shows that additional and strong three-dimensional perturbations were introduced in the boundary-layer by that notch. Their amplitude was approximately ten times as large as that of the amplitude of the perturbations usually detected upstream of separation ($\Delta p_p' = 60\%$ instead of 6%). Taking into account the size of the notch, it might be expected, by simple proportionality, that an indentation 10 times smaller would produce perturbations of the same intensity as the ones usually observed (6%) that is for a characteristic dimension of the notch of the order of $1/100$ mm or less. This was precisely the accuracy of the leading-edge of the various models that were used in the present research. An example is given in figure 8 (a-b), where the leading-edge thickness of model S-3 is given against the z -coordinate, as determined by a microscope; the vertical scale is enlarged by a factor of 500 over the horizontal scale, hence the saw-tooth appearance of the leading-edge.

Similar results are shown in figure 7b also related to model S-3. A notch approximately 40 microns deep, introduced a local change in $\Delta p_p'$ of about 22% .

The leading-edge effect was further examined by testing model S-6 (table I) which had a smaller leading-edge thickness than model S-3 (13 microns instead of 72 microns). Model S-6 which had a span equal to 150 mm and a step height of 3 mm, was tested with artificial irregularities in the leading-edge thickness. This was done by painting the lower surface of the leading-edge wedge along a small portion of the span, very close to the leading-edge itself. The boundary-layer was surveyed at $x = -25$ mm and $+44$ mm with and without that "thickness element". This is shown in figure 9; the corresponding leading-edge geometry is given in figure 10. Figure 9 shows that the thickness element introduced additional and strong

perturbations in the boundary-layer. At $x = -25$ mm, a local change of Δp_p of 12 % was recorded, while it was equal to 45 % after reattachment (i.e. at $x = 44$ mm). The local increase in leading-edge thickness was of about 20 microns, with the thickness element.

Effect of the machining accuracy of the leading-edge

From the results of the preliminary investigation, it seemed possible to conclude that the regular pattern of perturbations detected in the boundary-layer at reattachment was triggered by leading-edge irregularities. In these conditions, these irregularities should be smaller than 1 to 0.5 micron to maintain a two-dimensional flow within one percent assuming no other influence such as possible free-stream irregularities. In order to check these results further, it was decided to improve the machining accuracy of the leading-edge of the models and observe its effect on the flow perturbations.

With the available machine-tools, this was possible only by using smaller models. The length (L) of the flat plate, upstream of the step, and the span (S) were reduced to 80 mm and 200 mm instead of 225 mm and 400 mm respectively. The step-height was accordingly reduced to 6 or 7 mm, instead of 10 mm. In these circumstances, two identical models (except for the step-height) were machined which had a mean leading-edge thickness of 224 and 96 microns respectively, with an accuracy of 3 microns. As no straightforward comparison could be made between the results obtained on these two models and those already recorded on model S-3 (because of its different size), a third identical model was machined with the usual accuracy of 20 microns; it had a mean leading-edge thickness of 165 microns. Finally, provision was made to fix two small plates to the sides of the models, to check the influence of the reduced span. The configuration and designation of the models, are given in Table I (series S-20), the existence of side-plates being denoted by the symbol B. The mean thickness (ϵ_m) of the leading-edge is indicated in microns, as well as the magnitude of the local variation of thickness ($\Delta \epsilon$).

Discussion of the results

All the tests were made at a free-stream Mach number of 2.16 and a tunnel stagnation pressure of 150 mm Hg absolute, for which transition was located downstream of the reattachment region of the flow as shown by the schlieren pictures (figure 5-b). Total-head transverse surveys were made in the boundary-layer at a distance $x = 69$ mm downstream of the step base. A flat probe, higher than wider (outside dimensions 1.9 mm x 1 mm) was used which was more sensitive to detect the flow perturbations than the usual cylindrical probes; it was kept in contact with the model surface during its motion. The flow on the surface of the model was examined by the use of the sublimation technique and the geometry of the leading-edge was observed with a microscope.

Model S-20-e was tested under these conditions with and without the side-plates (B). The results are compared in figures 11.1 and 11.2. The removal of the side-plates influenced the perturbations, inasmuch as their amplitude decreased by about 50 %. It also resulted in an increase of the base pressure (as measured directly or as shown by the position of the expansion fan on the schlieren pictures; figures 5-b and 5-c) and in a decrease of the pitot-pressure measured on the center-line of the model at $x = 69$ mm. This proved that a certain amount of air was injected in the separated flow from the sides of the model when the side-plates were removed.

With the side-plates, the local variations of Δp_p^l measured between a pressure peak and its neighbouring valley, varied between 20 and 54 %, with a mean value of 25 %. The leading-edge geometry is shown in figure 8-c; its mean thickness was 165 ± 45 microns over the entire span of the model and local variations in thickness were of about 20 microns at most. Assuming that the flow perturbations were triggered by leading-edge irregularities, the latter should be of the order or less than 1 micron to maintain a two-dimensional flow within one percent. These results agree quantitatively with the conclusions obtained from testing model S-3 and were therefore used as a reference for the effect of improving the accuracy of machining

of the leading-edge.

Figure 11 (1 and 2) also shows that the wave-length of the flow perturbations was not affected by the removal of the side-plates (that is by the model span) verifying the conclusions obtained in reference 1. The distance between successive peaks of the total-head distribution varied between 3 and 6 (figure 11), with a mean value of 4.2 mm.

Flow perturbations are also shown in figure 12 for models S-20-e and S-20-e-(B) where regions of high sublimation rates correspond to dark areas. It is easy to see that the wave-length is the same on both models and also that the perturbations are stronger in the presence of side plates. Note that the leading-edge plate was not coated with azobenzene, but only the surface on which reattachment occurred, to avoid a modification of the roughness of the surface.

Models S-20-f and S-20-c have been tested under the same conditions as model S-20-e. The amplitude of the perturbations was again reduced by the removal of the side plates. Only the results obtained with the side-plates are shown in figure 11 (3 and 4) and compared with the pressure variations measured on model S-20-e-(B) at the same value of x (i.e. 69 mm). It is seen that the amplitude of the flow perturbations has been drastically reduced. The mean value of the local change in Δp_p was indeed reduced to about 6.5 % for both models instead of 25 % on model S-20-e-(B), as the local variations in leading-edge thickness were reduced to 3 microns instead of 20 microns on model S-20-e-(B). Assuming proportionality, and that no other effect than that of leading edge irregularities, it is to be expected that a two-dimensional flow could be maintained within 1 % ($\Delta p_p = 1 \%$) if the leading-edge irregularities were smaller than 1 to 1/2 micron.

Figures 12-c and b show the striation pattern obtained on the surface of models S-20-c and S-20-f by the sublimation technique. Comparison with figure 12-b shows that the amplitude of the perturbations was reduced.

The wave-length of the flow perturbations was measured on the pressure distributions of figures 12-c-d. It varied between 3 and 6 mm on model S-20-f-(B) and between 2 and 6 mm on model S-20-c-(B), with mean values of 4.4 mm and 3.8 mm respectively. Therefore, within the accuracy of measurement, the wave-length remained unchanged (about 4 mm) as the intensity of the perturbations was reduced by improving the leading-edge accuracy. The observation of the models with the microscope never revealed a regular distribution of leading-edge irregularities. Furthermore, the leading-edges of greater accuracy were machined by different methods, from those of lower accuracy; so that even if such a regular distribution existed, it could not have been systematically the same on all the models. Therefore, the existence of leading-edge irregularities cannot explain the presence of a regular pattern of flow perturbations at reattachment. It is most probably a fundamental boundary-layer instability which in these tests is triggered by the leading-edge irregularities.

It is recognized that additional investigations remain to be done to determine exactly where the perturbations start to be regularly distributed. Without such information it is impossible to evaluate the flow curvature which is necessary to discuss the results in relation to Görtler's theory. Hopkins showed (Ref. 3) that the curvature existing at reattachment was two orders of magnitude greater than the minimum value required by Görtler and he concluded that the curvature required to produce vortices was so slight that this degree of curvature might even exist at the leading-edge. Therefore the large amplification of the intensity of the perturbations in the separated boundary-layer remains to be explained.

CONCLUSIONS

The flow perturbations extend, after reattachment, into the full thickness of the boundary-layer with a maximum intensity of pitot-pressure variations occurring at about mid-height, both in the laminar and turbulent portions of the boundary-layer. These variations vanish at the outer-edge

of the boundary-layer and have their maximum amplitude in the transition region.

Although the existence of a regular pattern of flow perturbations could not be explained by the presence of leading-edge irregularities, it appears that the boundary-layer instability was triggered by these irregularities. No relation existed between the spacing (i.e. the wave-length) of the flow perturbations and the distribution of leading-edge irregularities, however, the amplitude of the perturbations was approximately proportional to the size of these irregularities. By extrapolation of the results it is concluded that a two-dimensional boundary-layer flow might be obtained within one percent (in Δp_p) at reattachment, if the leading-edge thickness were constant to within 1/2 to 1 micron, assuming no other effect such as the influence of possible irregularities in the flow.

REFERENCES

1. J.J. Ginoux - Laminar separation in supersonic flow with emphasis on three-dimensional perturbations at reattachment.
T.C.E.A. TN 3 - February 1960.
2. J.J. Ginoux - The T.C.E.A. continuous supersonic wind tunnel S-1,
T.C.E.A. TM 7-October 1960.
3. E.J. Hopkins, S.J. Keating and A. Bandettini - Photographic evidence of streamwise arrays of vortices in boundary-layer flow,
NASA TN D-328 - September 1960.

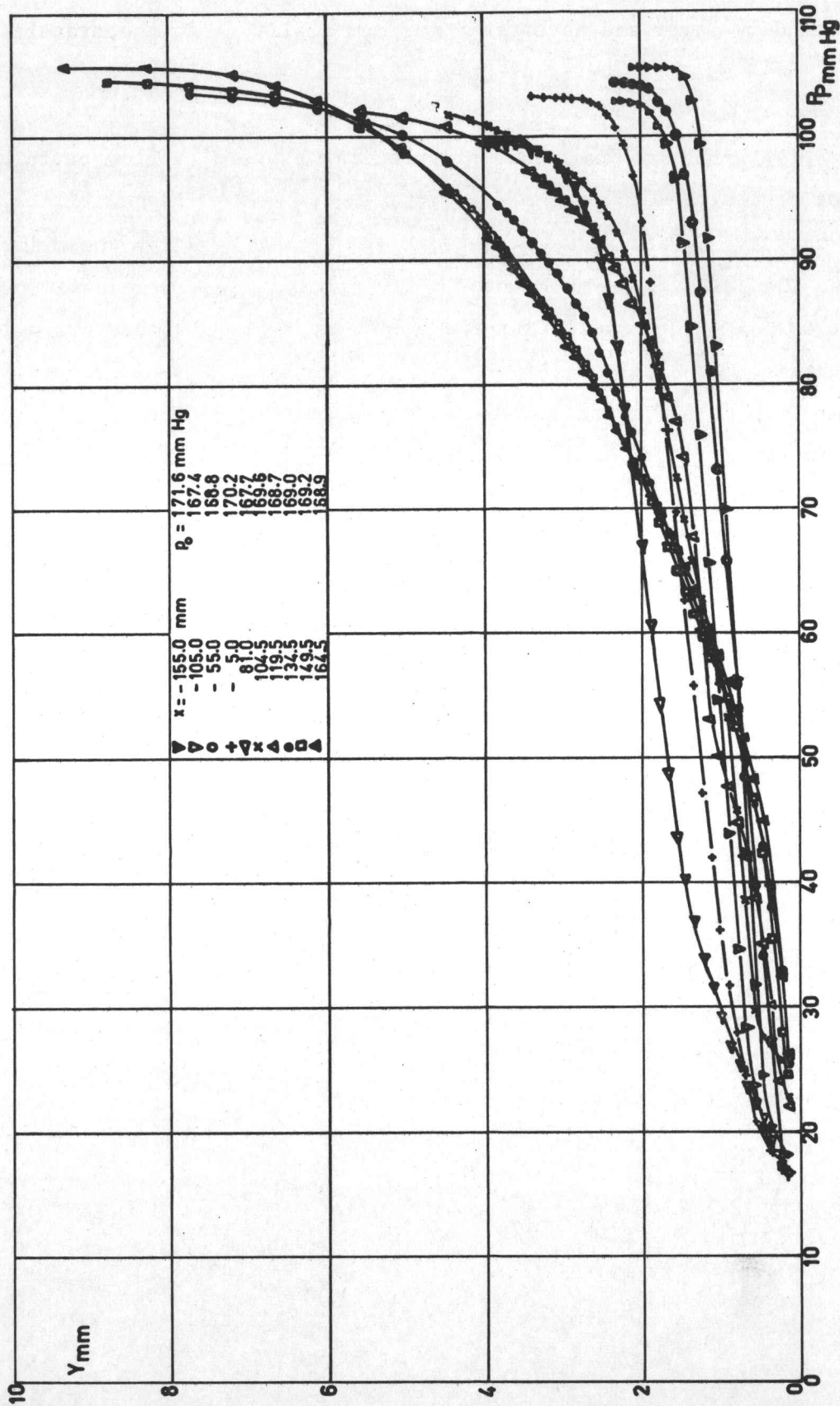


FIGURE 1 - MODEL S-3 = pitot-pressure profiles at various x on model centre-line

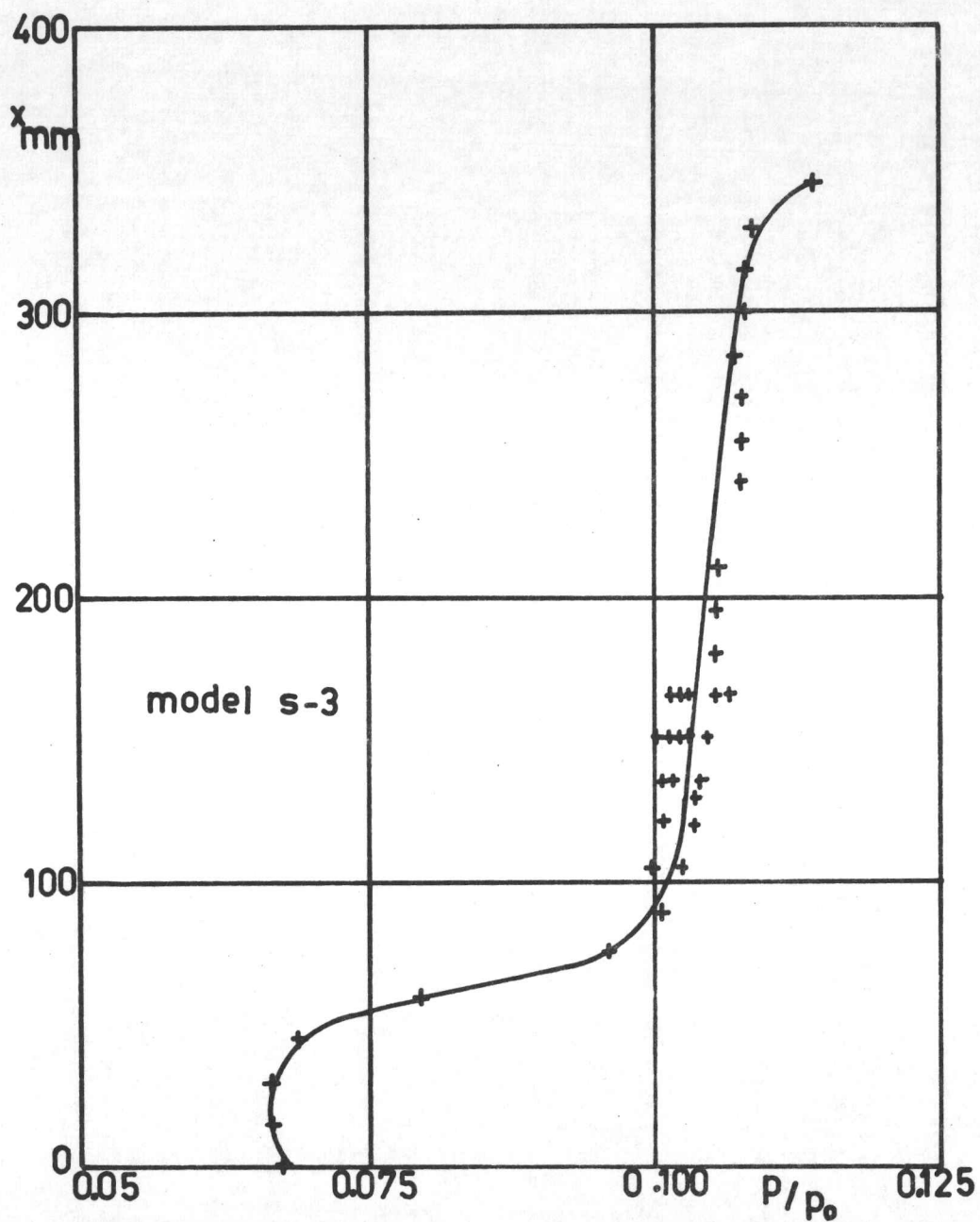


FIGURE 2 - Static pressure distribution on the axis of the model

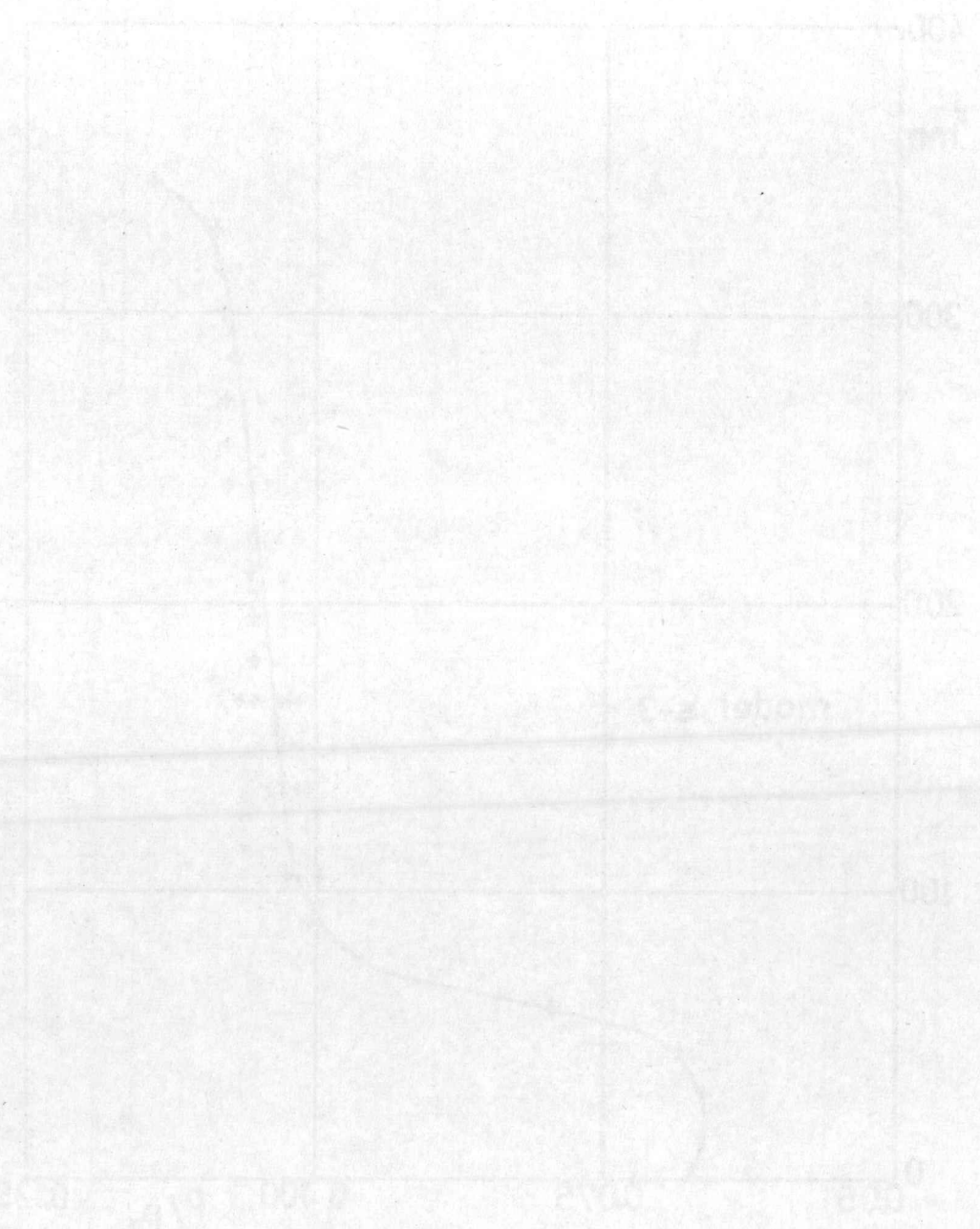


FIGURE 2.1. Static pressure distribution on the axis of the model.

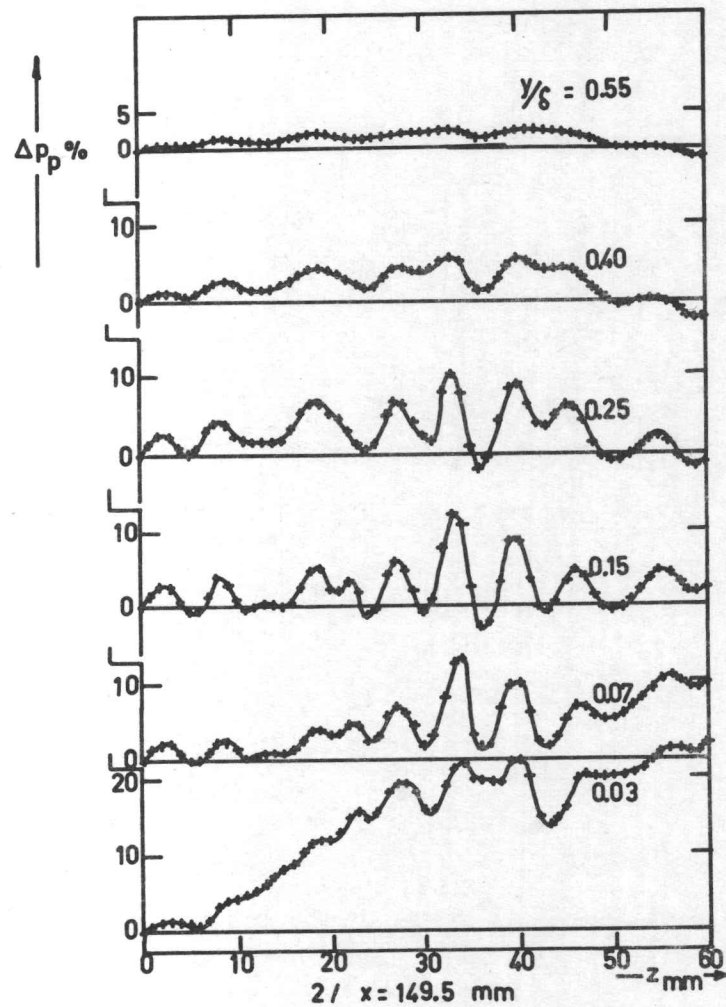
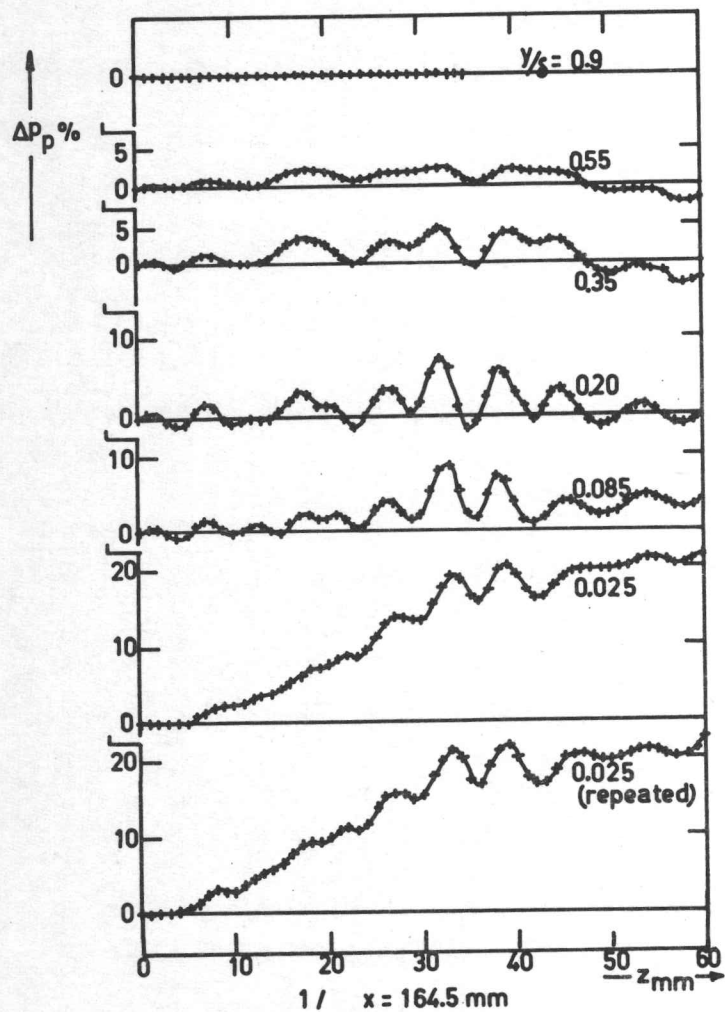
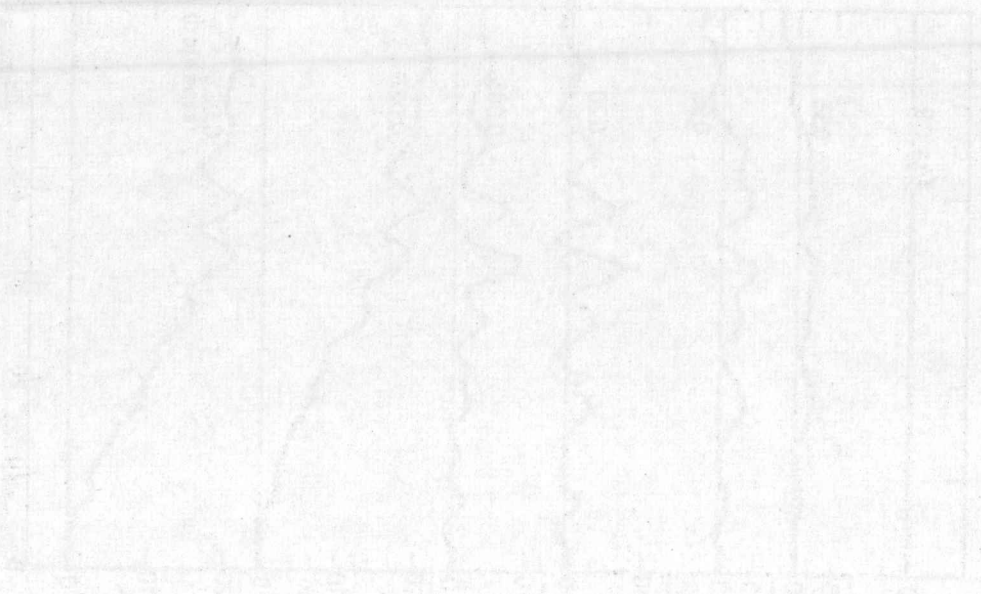
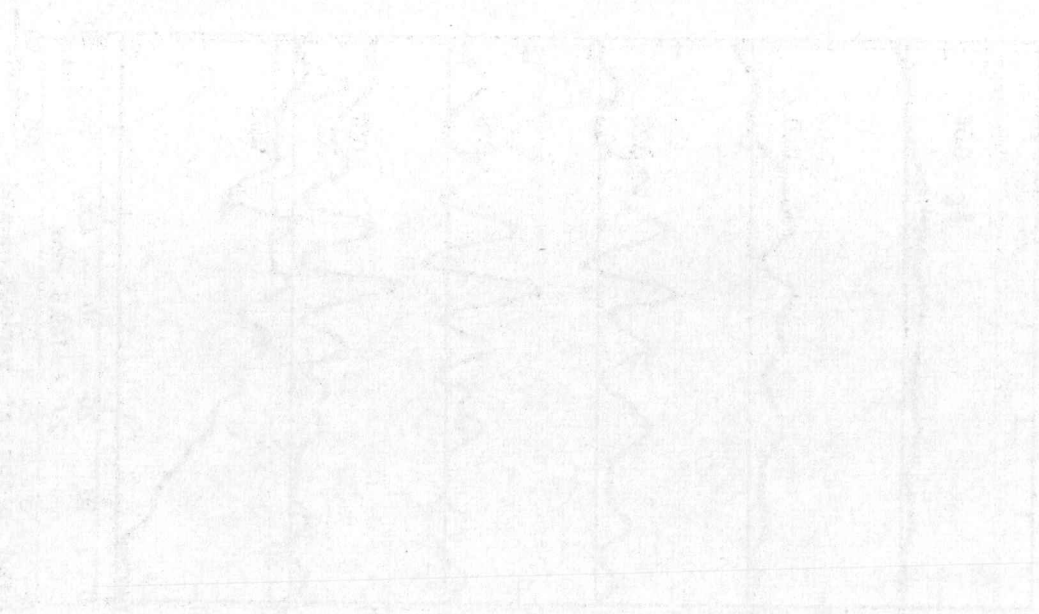


FIGURE 3 - transverse surveys

with a total head probe at various x and y
MODEL S-3



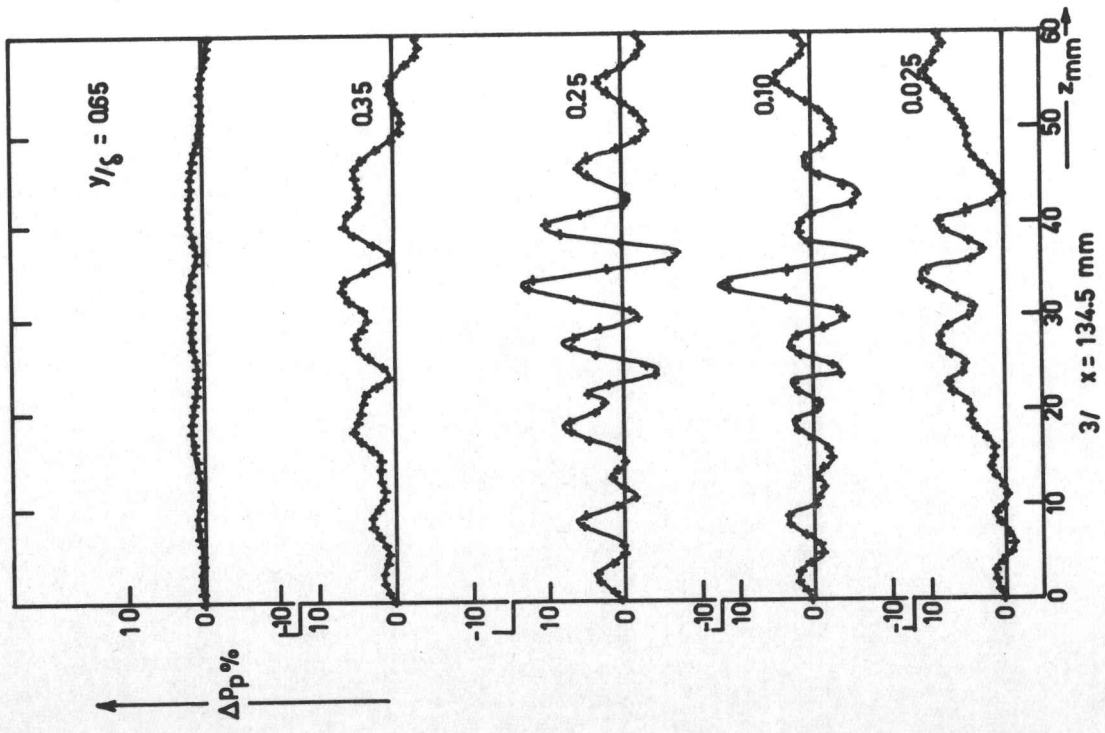
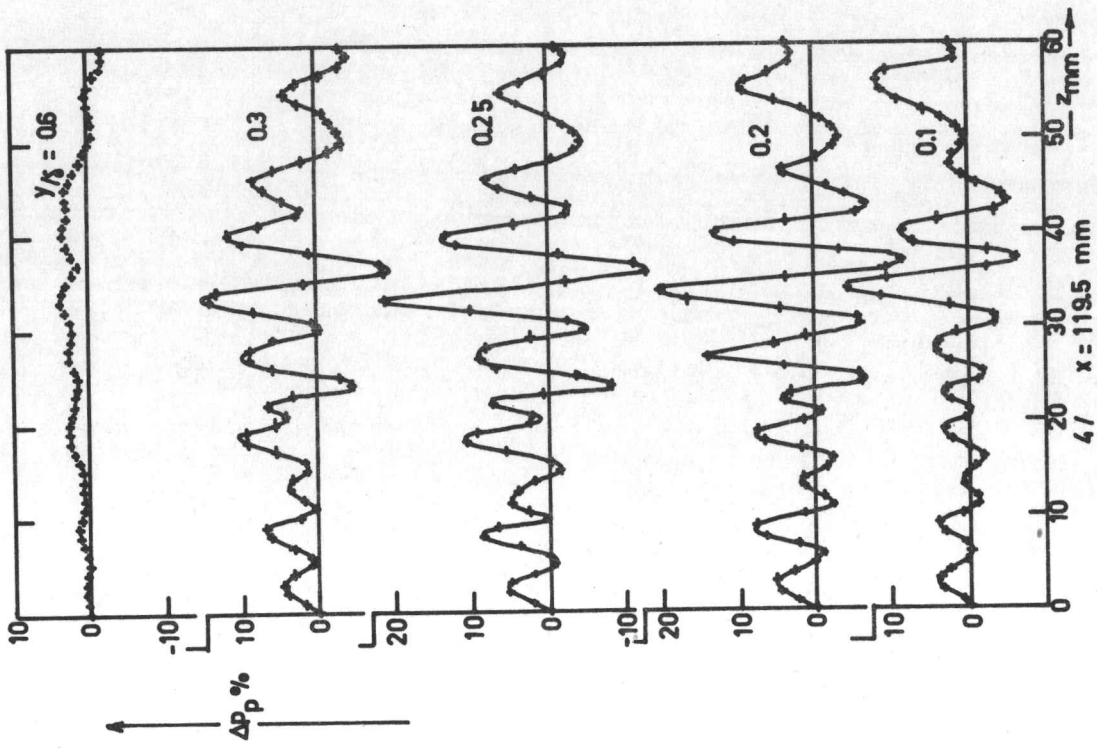
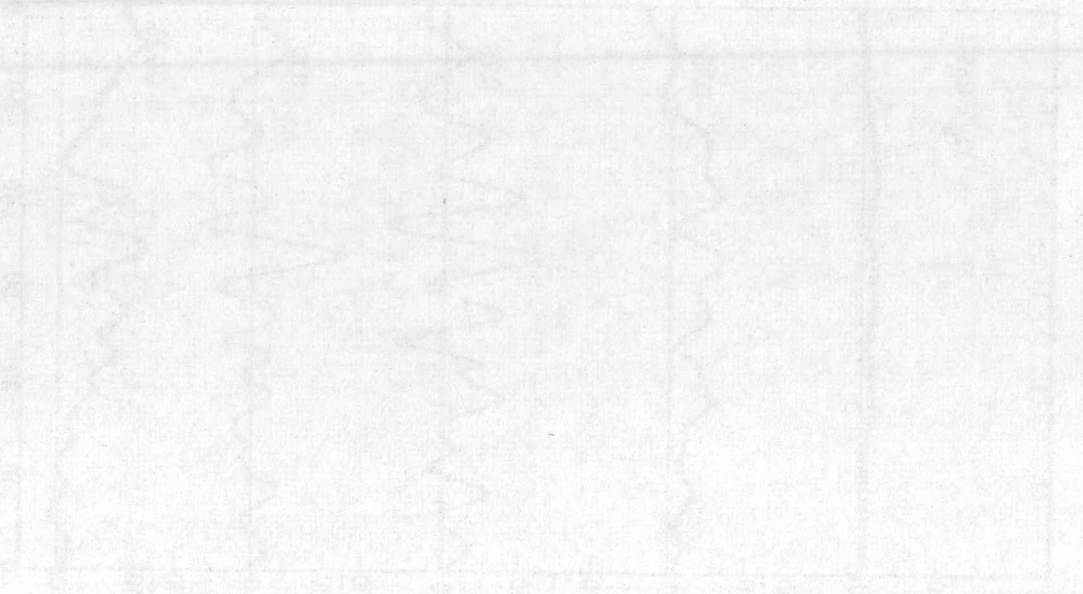
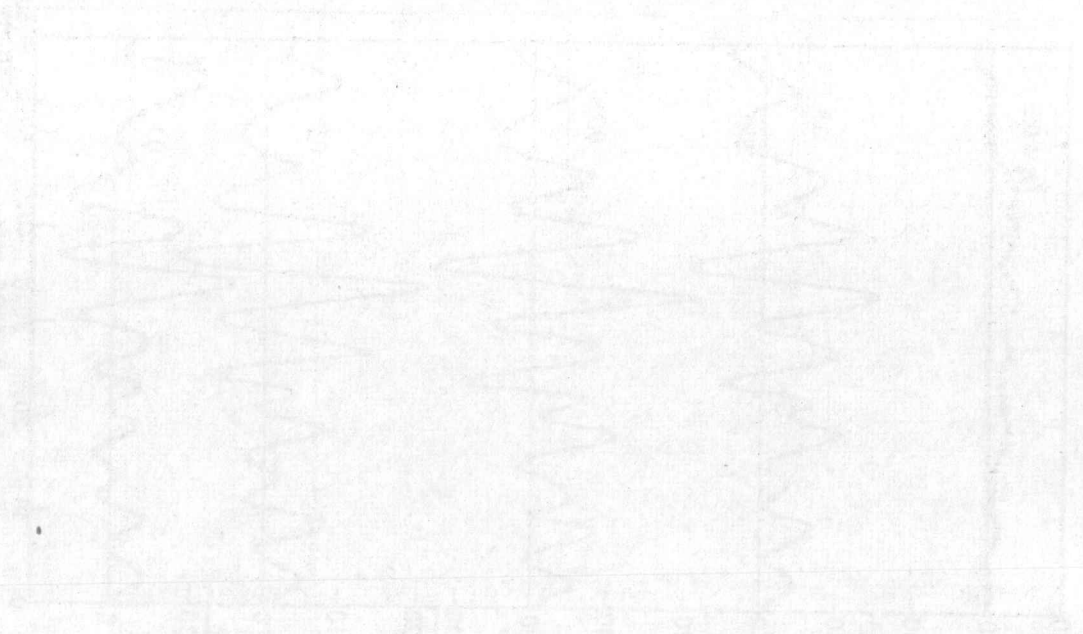


FIGURE 3 - Continued



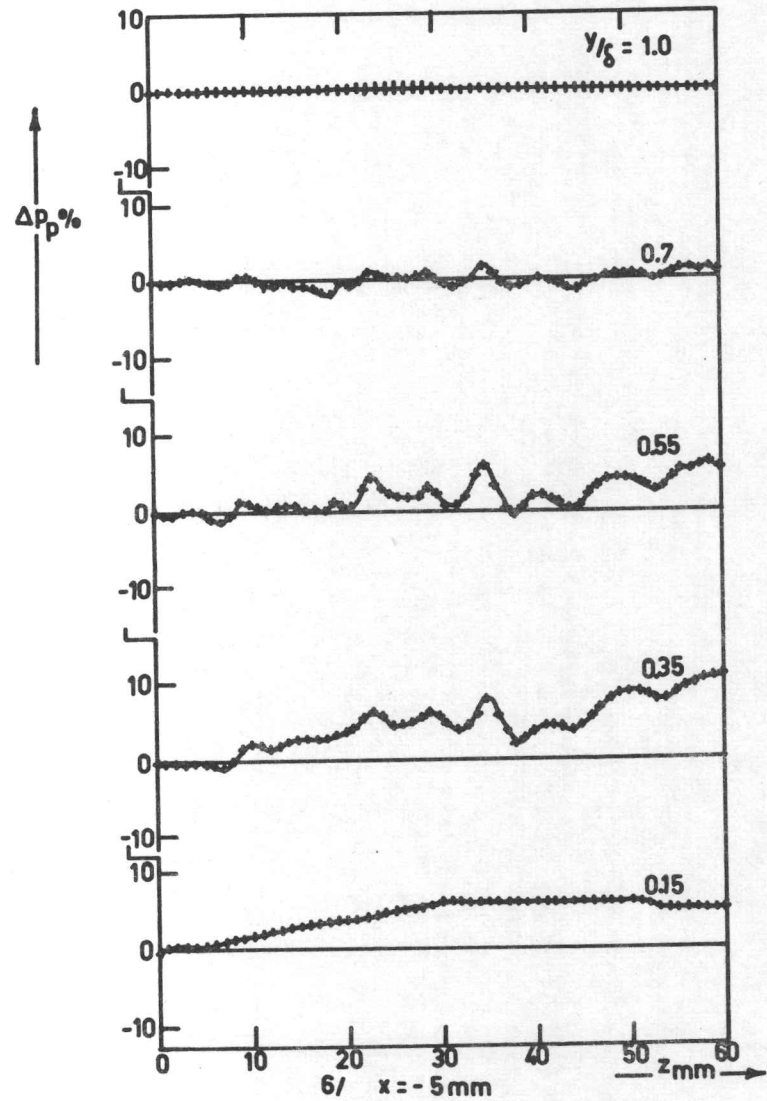
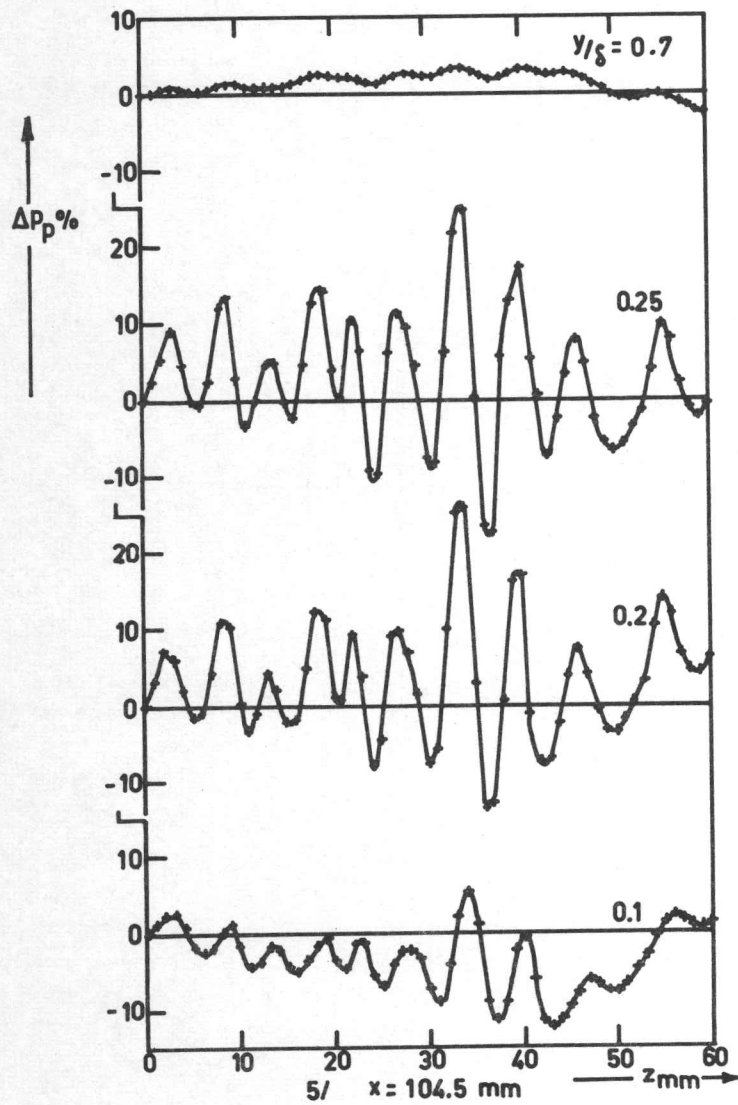
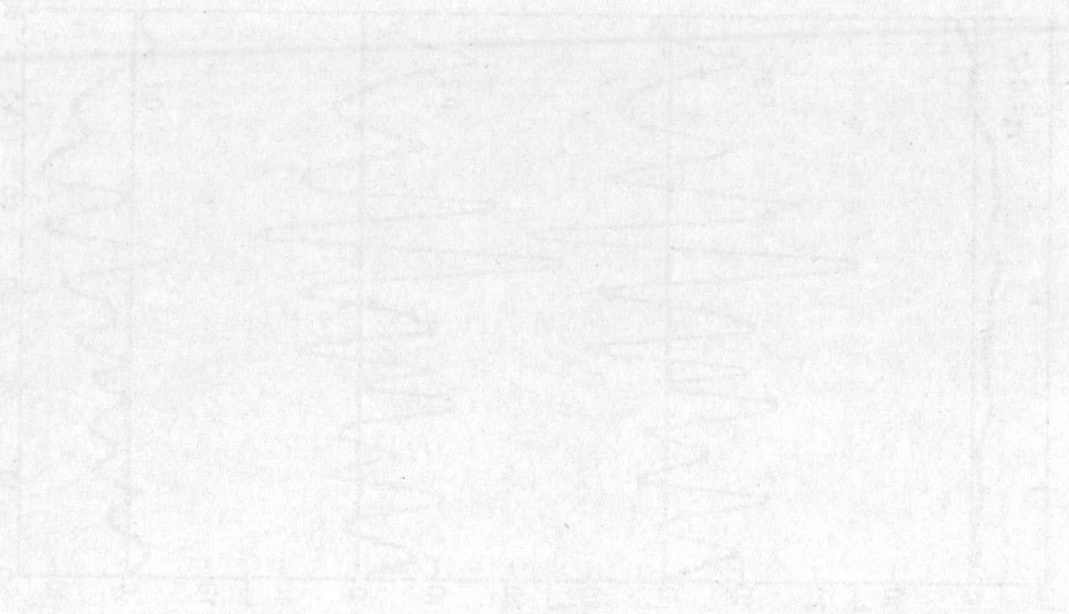
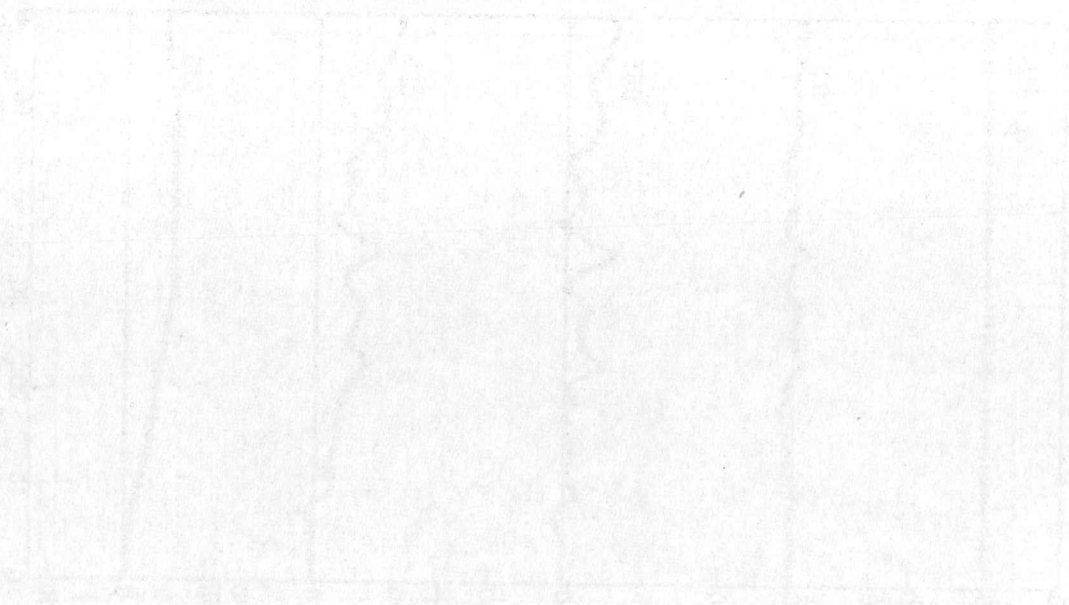


FIGURE 3 - Continued



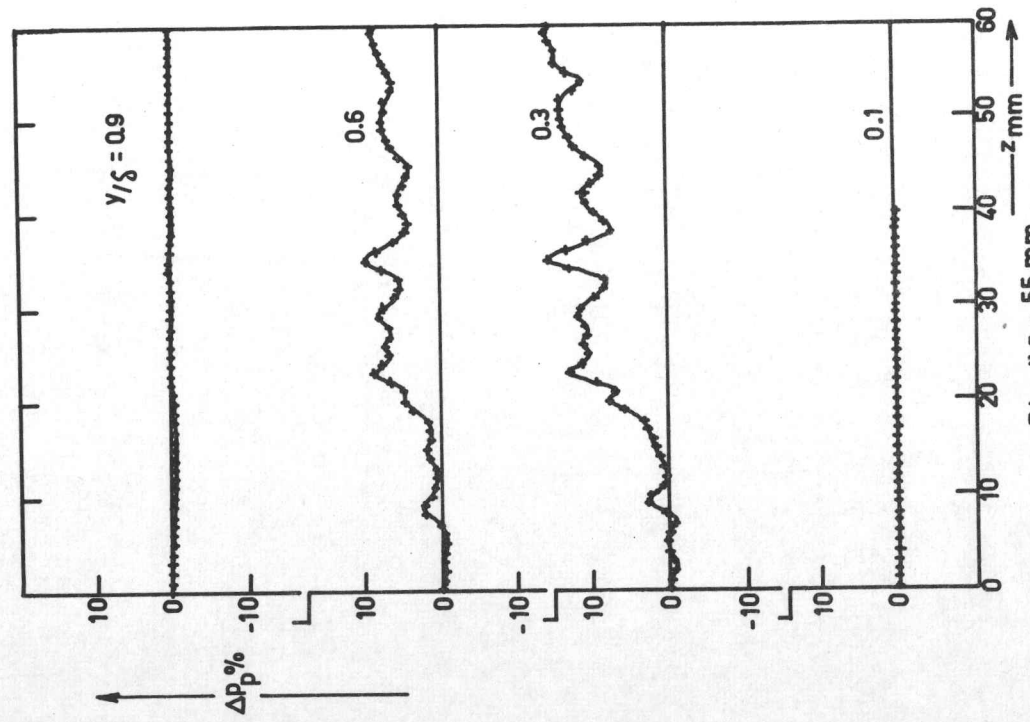
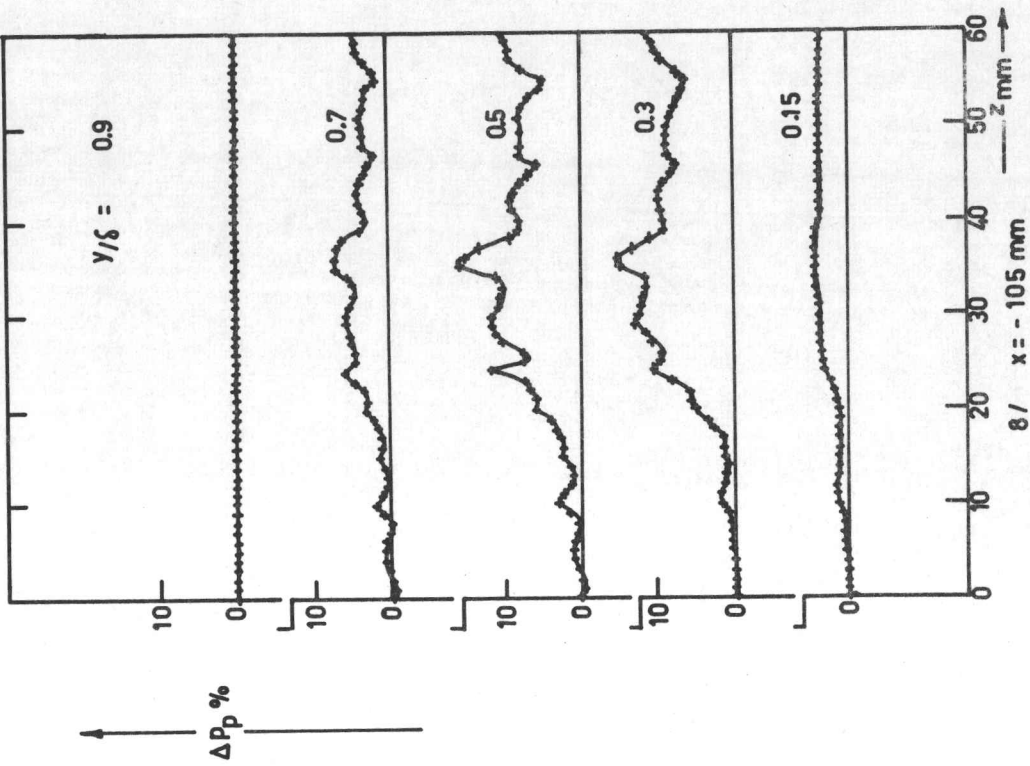
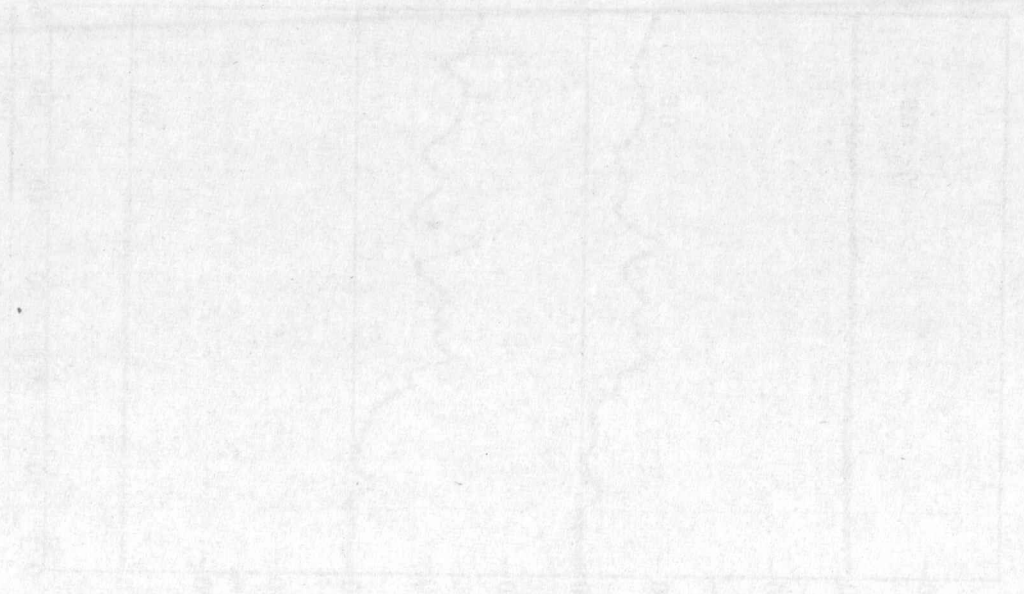
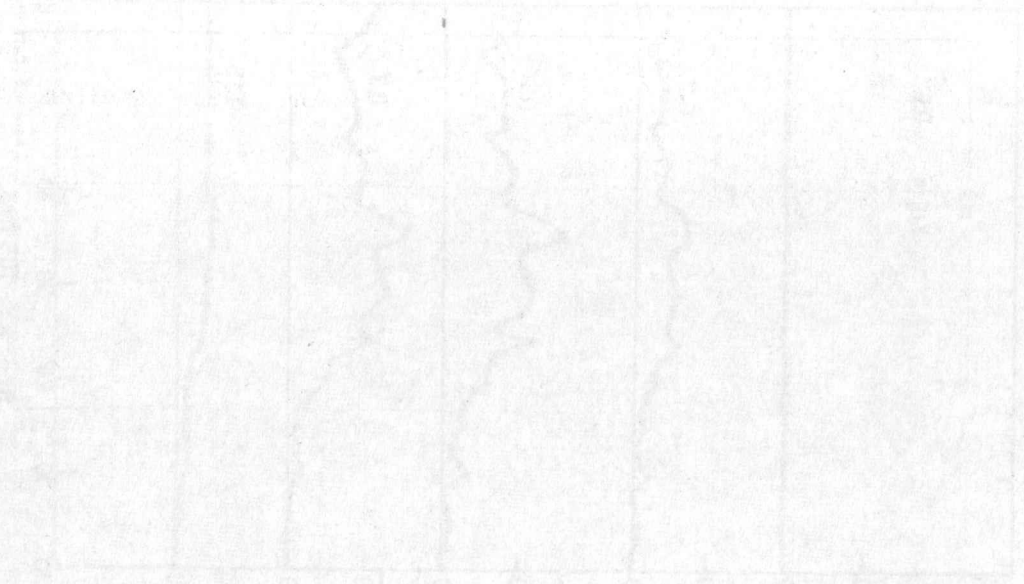


FIGURE 3 - Continued



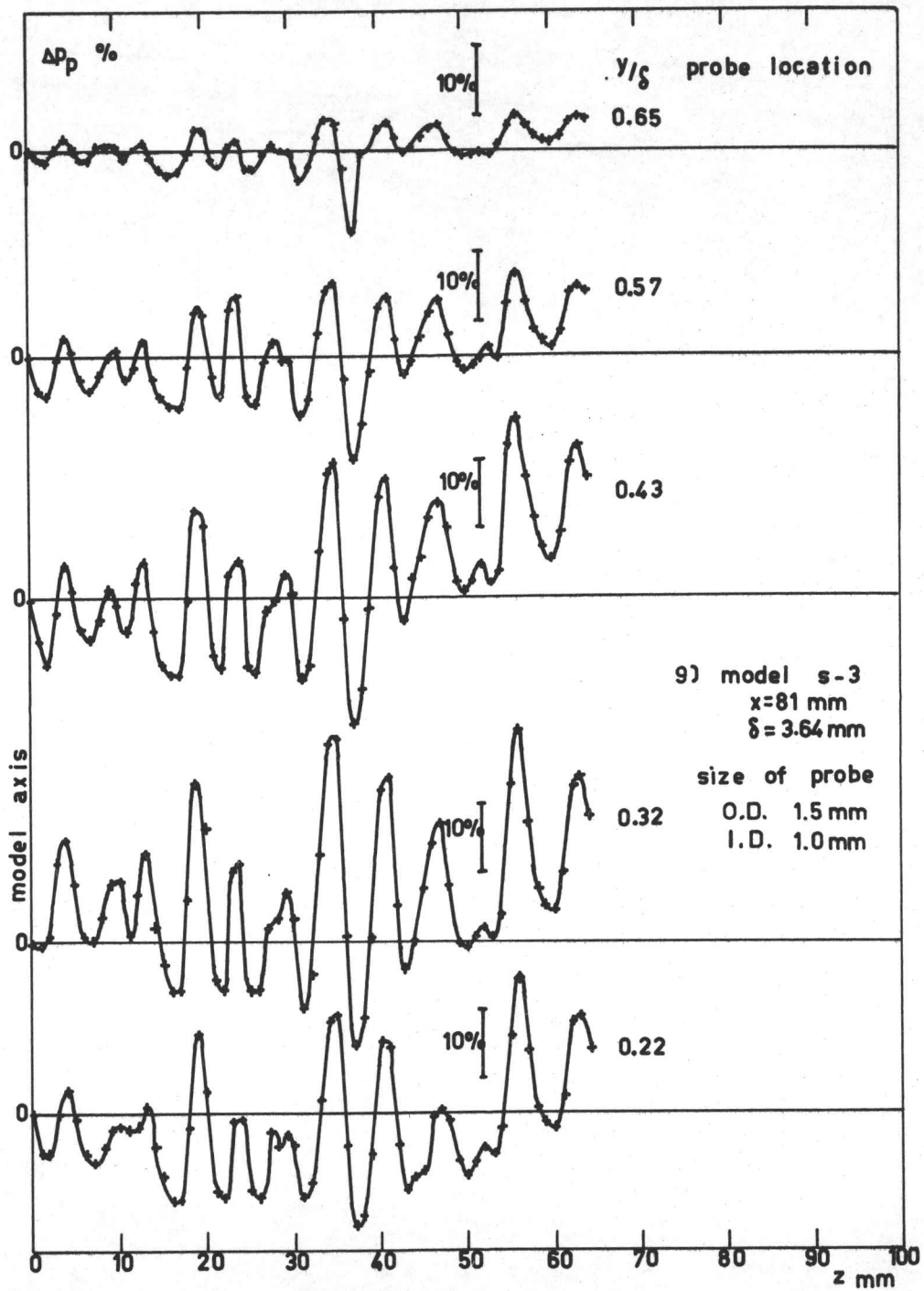


FIGURE 3 - continued



1.0
 2.0
 3.0
 4.0
 5.0

FIGURE 4 - 7-11-50

DATE	DESCRIPTION	AMOUNT	CHECK NO.	BANK
10/1/58	STATE OF TEXAS	100.00		FIRST NATIONAL BANK
10/2/58	STATE OF TEXAS	100.00		FIRST NATIONAL BANK
10/3/58	STATE OF TEXAS	100.00		FIRST NATIONAL BANK
10/4/58	STATE OF TEXAS	100.00		FIRST NATIONAL BANK
10/5/58	STATE OF TEXAS	100.00		FIRST NATIONAL BANK
10/6/58	STATE OF TEXAS	100.00		FIRST NATIONAL BANK
10/7/58	STATE OF TEXAS	100.00		FIRST NATIONAL BANK
10/8/58	STATE OF TEXAS	100.00		FIRST NATIONAL BANK
10/9/58	STATE OF TEXAS	100.00		FIRST NATIONAL BANK
10/10/58	STATE OF TEXAS	100.00		FIRST NATIONAL BANK
10/11/58	STATE OF TEXAS	100.00		FIRST NATIONAL BANK
10/12/58	STATE OF TEXAS	100.00		FIRST NATIONAL BANK
10/13/58	STATE OF TEXAS	100.00		FIRST NATIONAL BANK
10/14/58	STATE OF TEXAS	100.00		FIRST NATIONAL BANK
10/15/58	STATE OF TEXAS	100.00		FIRST NATIONAL BANK
10/16/58	STATE OF TEXAS	100.00		FIRST NATIONAL BANK
10/17/58	STATE OF TEXAS	100.00		FIRST NATIONAL BANK
10/18/58	STATE OF TEXAS	100.00		FIRST NATIONAL BANK
10/19/58	STATE OF TEXAS	100.00		FIRST NATIONAL BANK
10/20/58	STATE OF TEXAS	100.00		FIRST NATIONAL BANK
10/21/58	STATE OF TEXAS	100.00		FIRST NATIONAL BANK
10/22/58	STATE OF TEXAS	100.00		FIRST NATIONAL BANK
10/23/58	STATE OF TEXAS	100.00		FIRST NATIONAL BANK
10/24/58	STATE OF TEXAS	100.00		FIRST NATIONAL BANK
10/25/58	STATE OF TEXAS	100.00		FIRST NATIONAL BANK
10/26/58	STATE OF TEXAS	100.00		FIRST NATIONAL BANK
10/27/58	STATE OF TEXAS	100.00		FIRST NATIONAL BANK
10/28/58	STATE OF TEXAS	100.00		FIRST NATIONAL BANK
10/29/58	STATE OF TEXAS	100.00		FIRST NATIONAL BANK
10/30/58	STATE OF TEXAS	100.00		FIRST NATIONAL BANK
10/31/58	STATE OF TEXAS	100.00		FIRST NATIONAL BANK

STATE OF TEXAS
 COUNTY OF DALLAS
 DEPARTMENT OF REVENUE
 RECEIVED

10/31/58

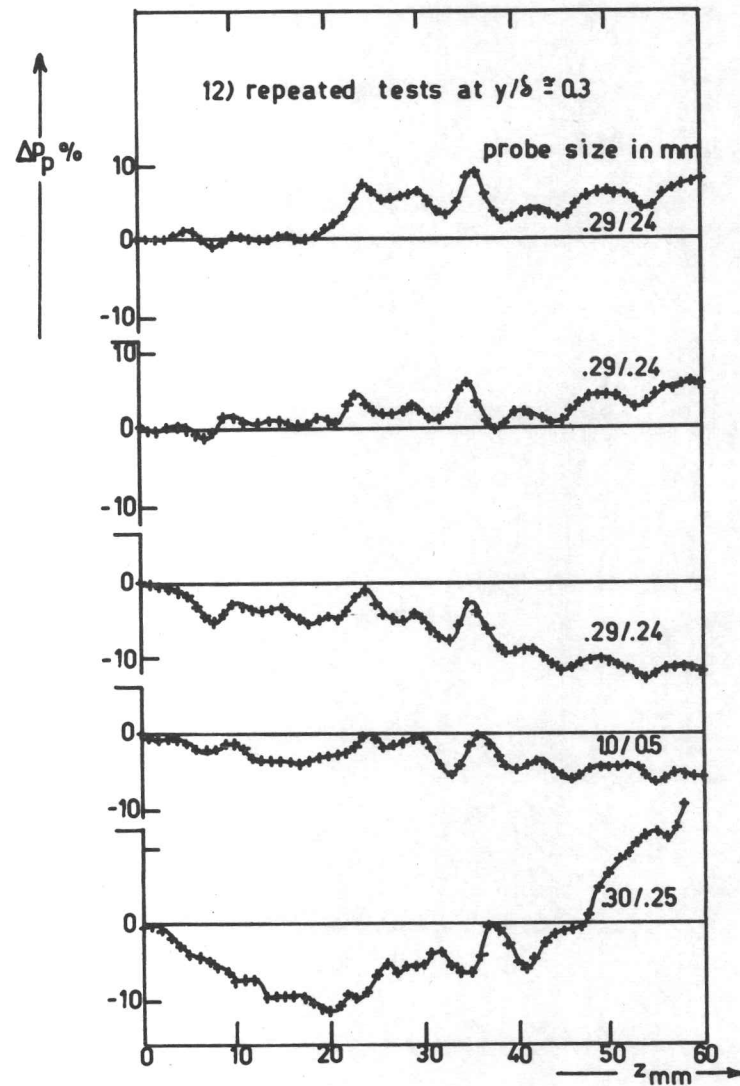
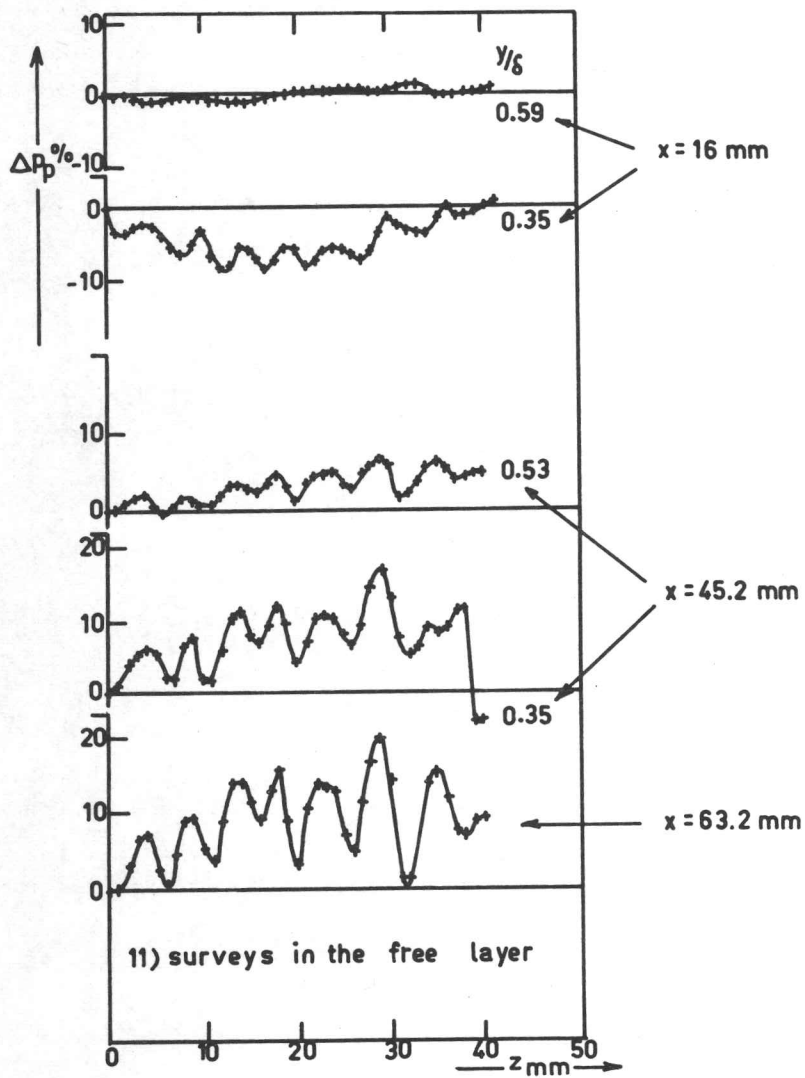
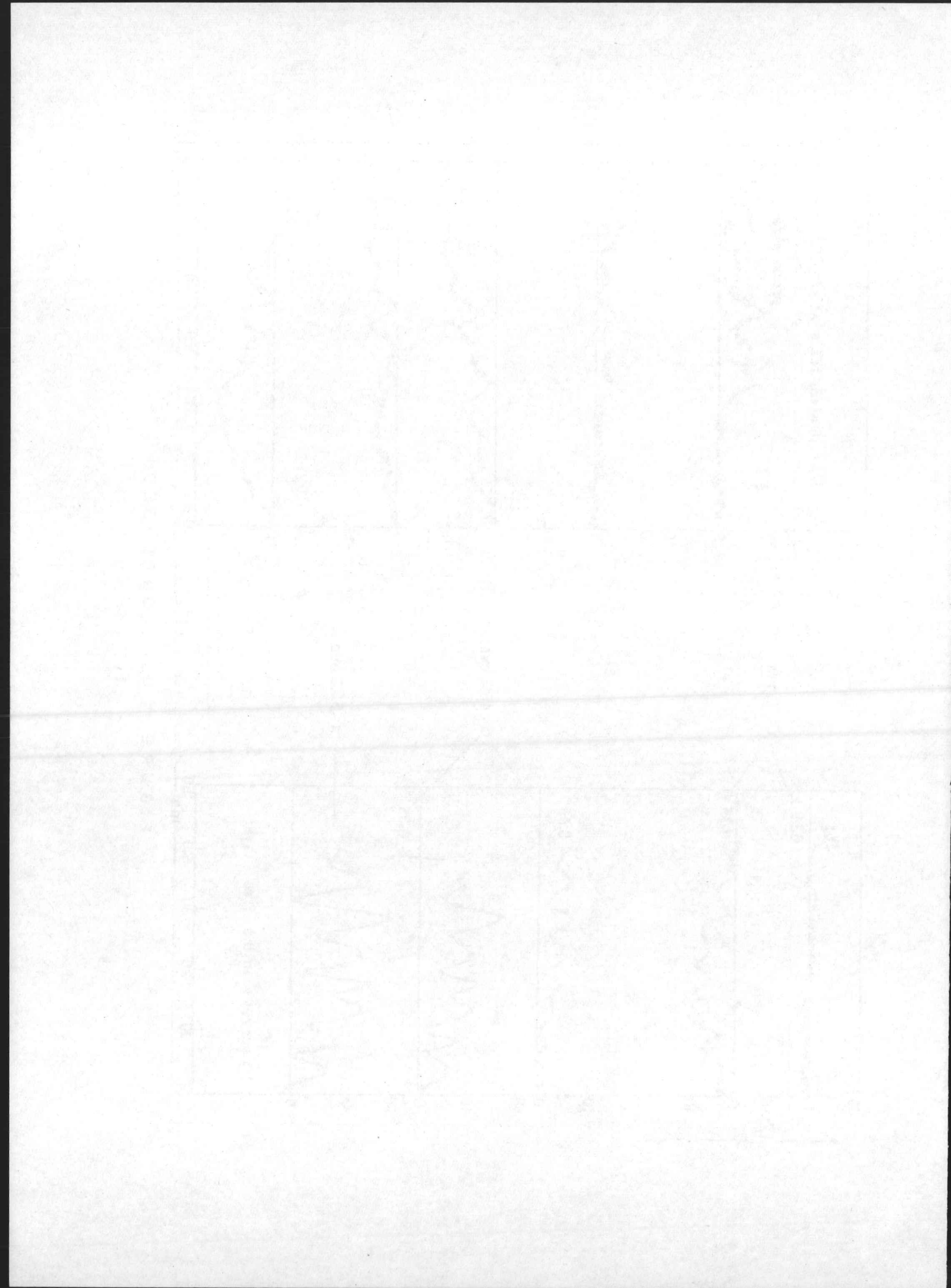


FIGURE 3 - CONCLUDED



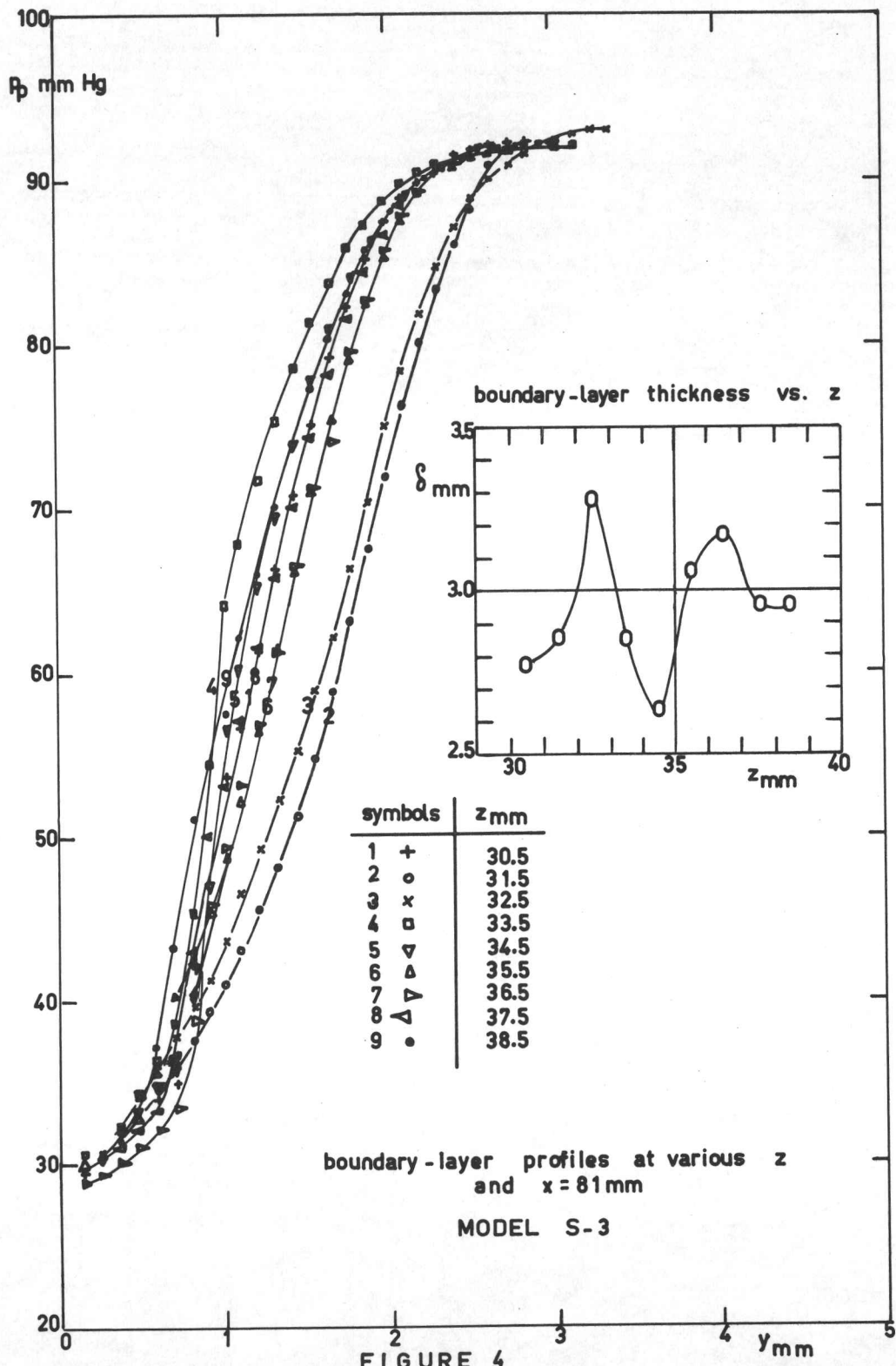


FIGURE 4

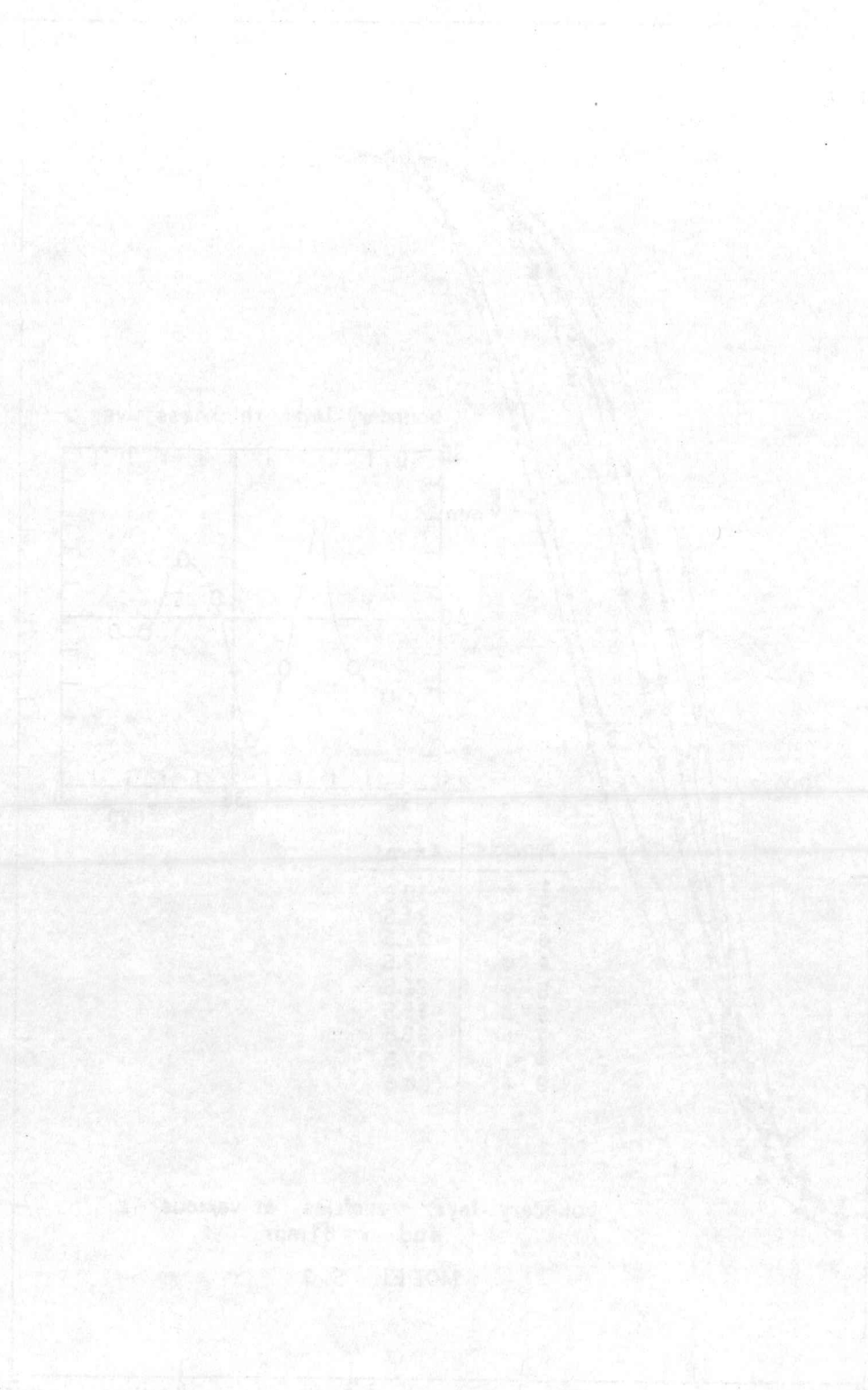
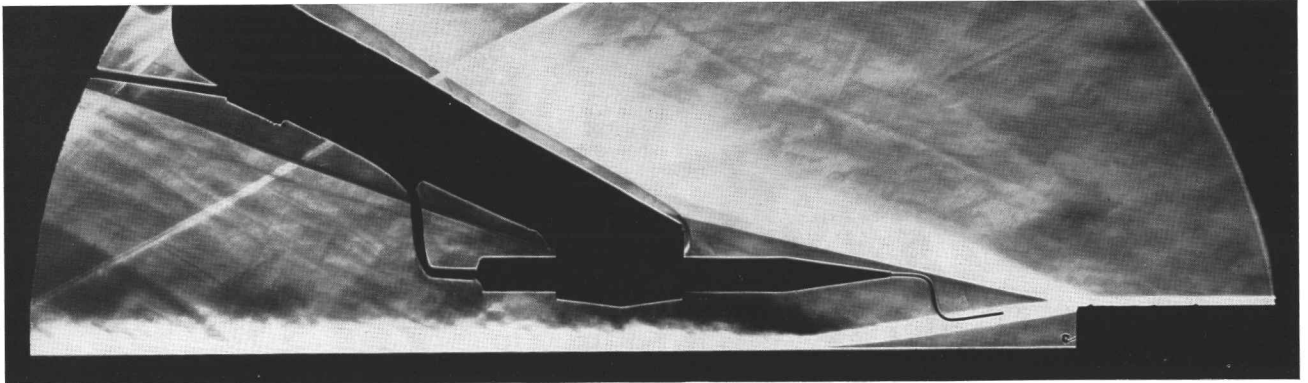
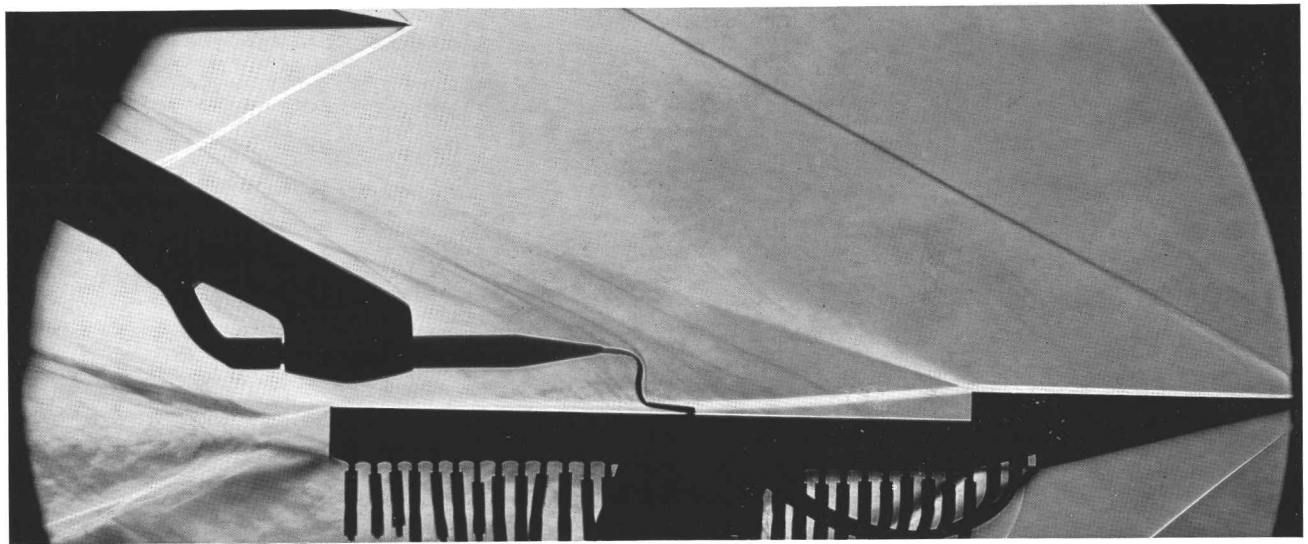


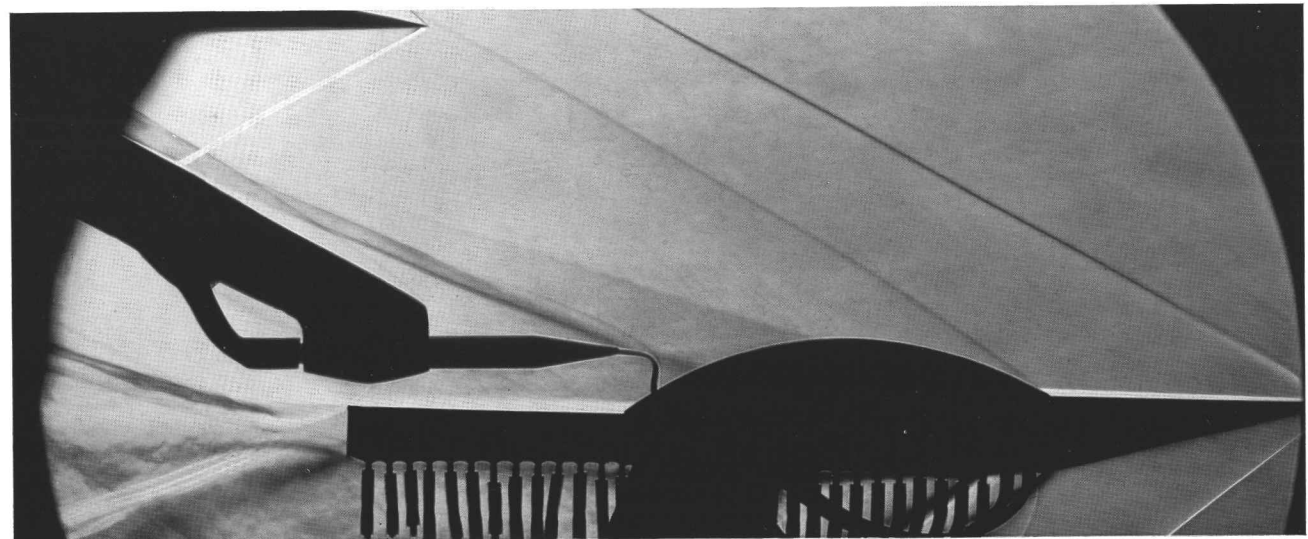
FIGURE 1



a) Model S-3

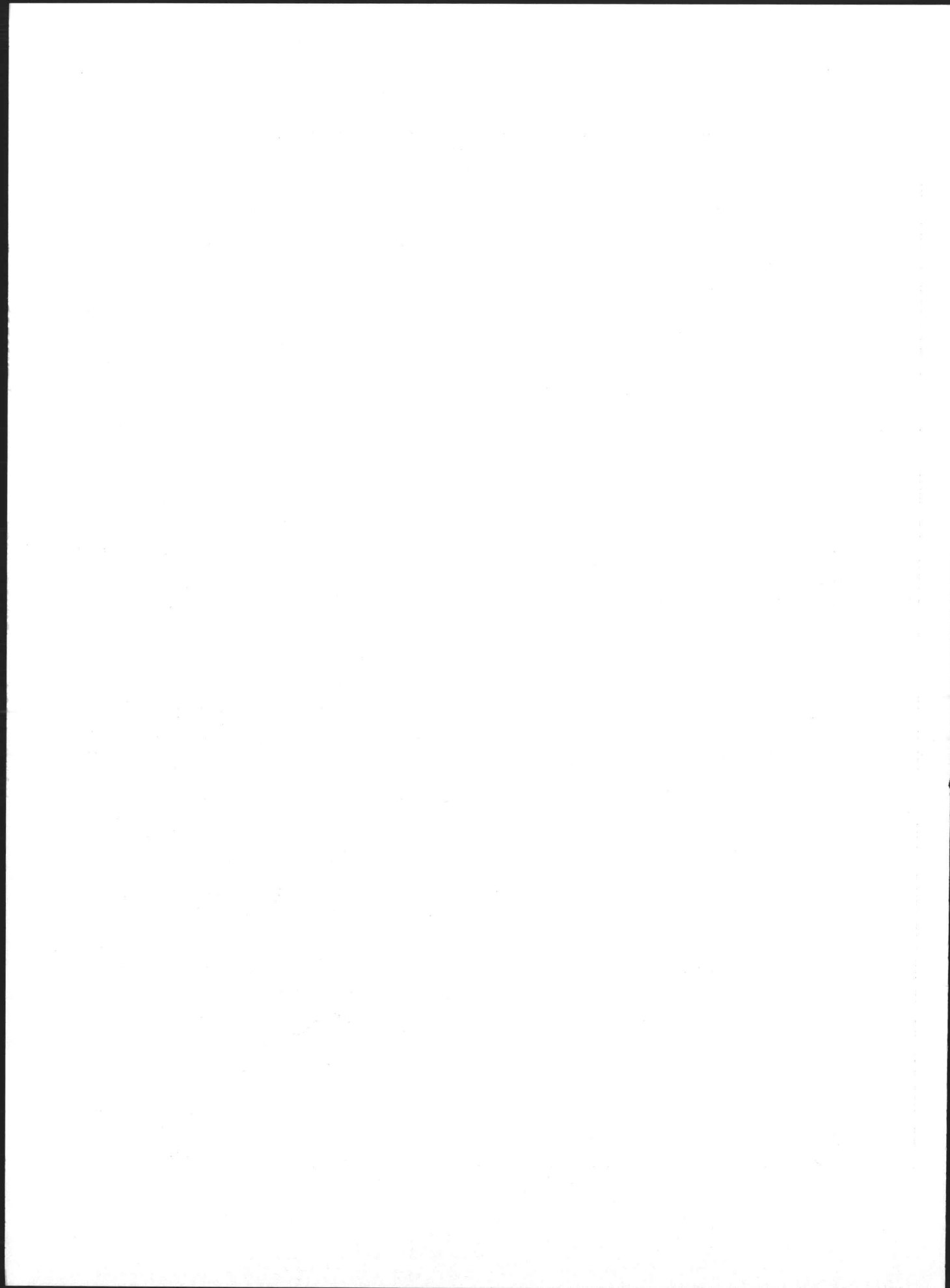


b) Model S-20-e



c) Model S-20-e-B

Figure 5. Schlieren photographs



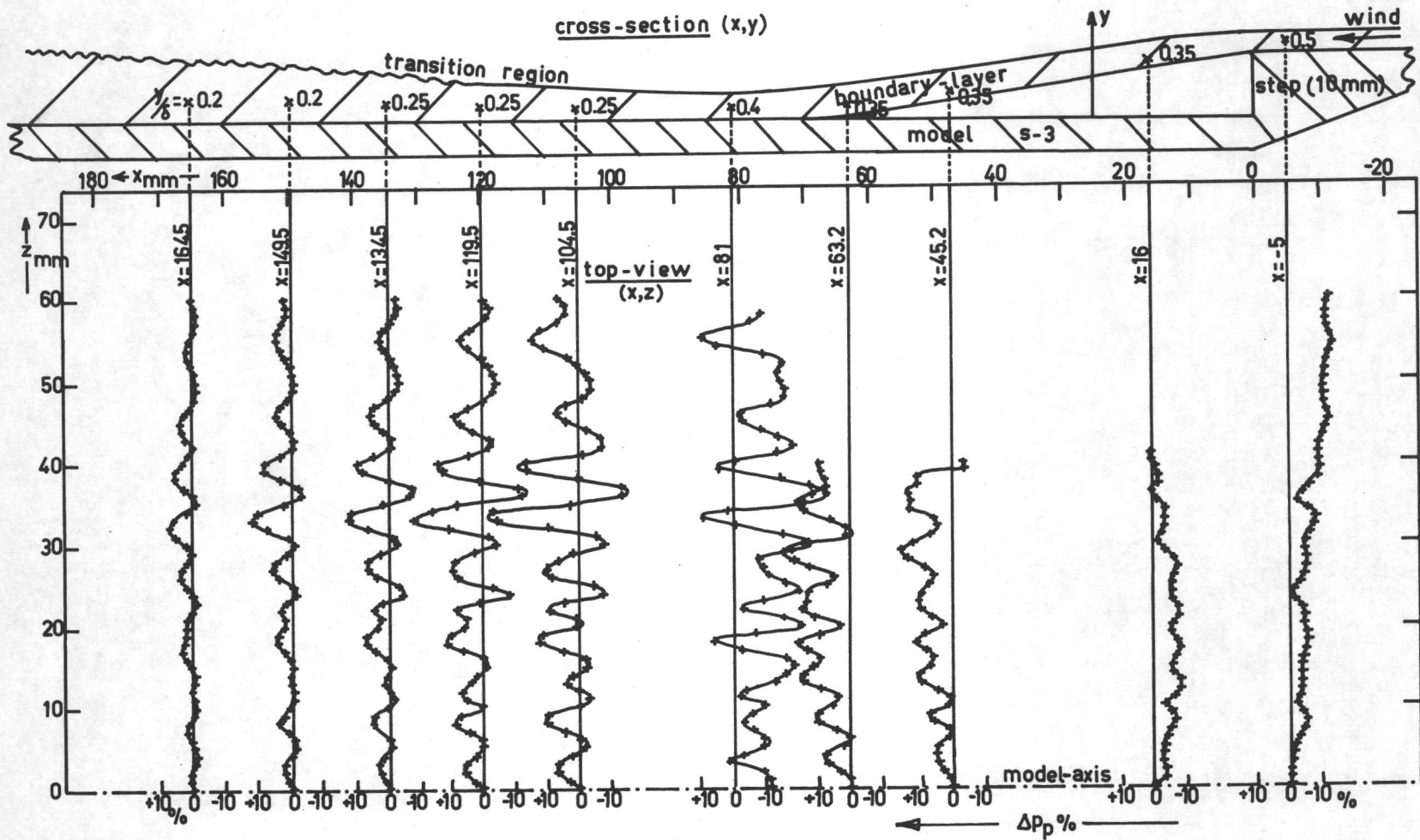


FIGURE 6-a - transverse variation of pitot-pressure at various x, in % of the pitot-pressure on model-axis. measurements downstream of the step

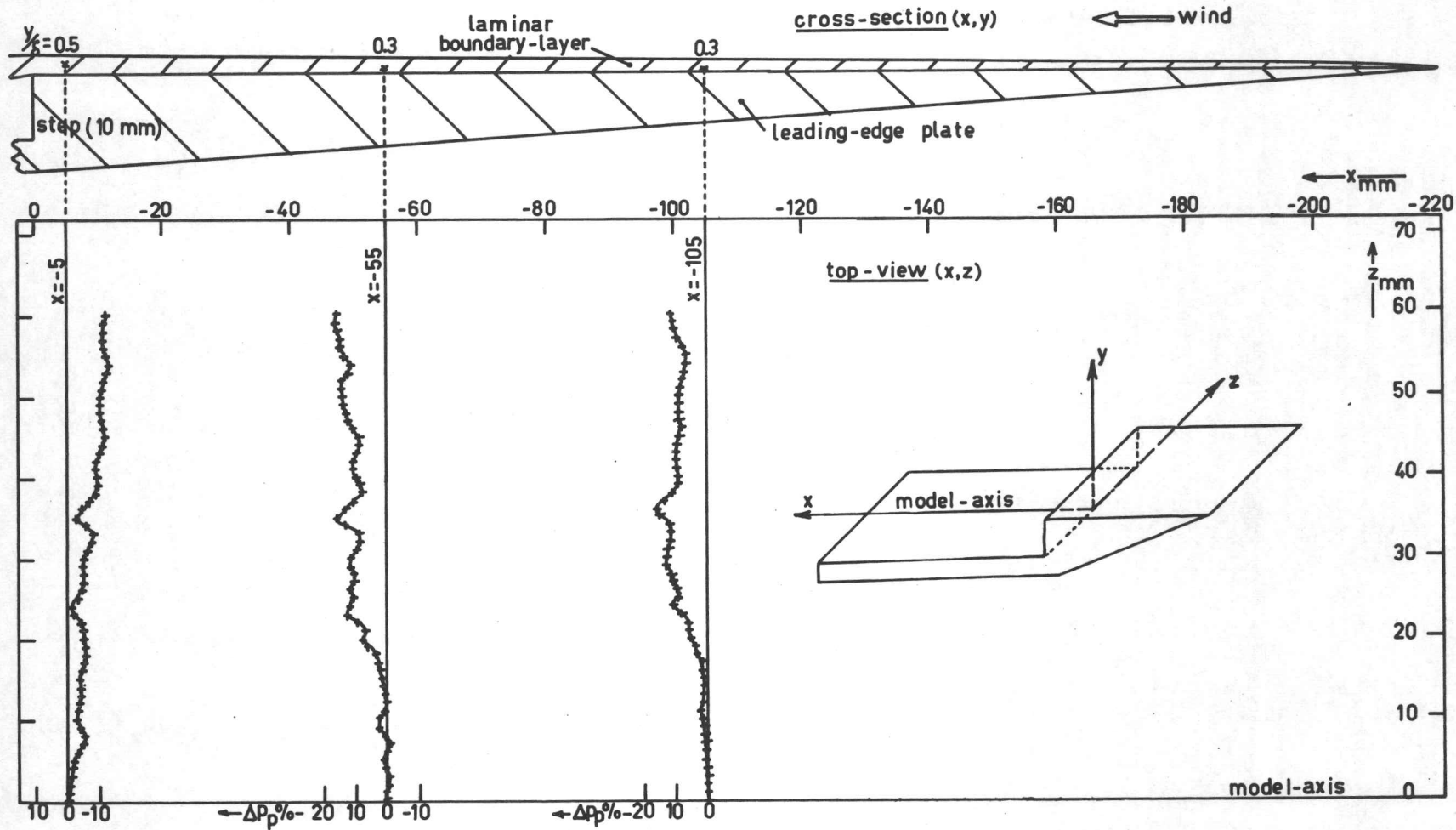
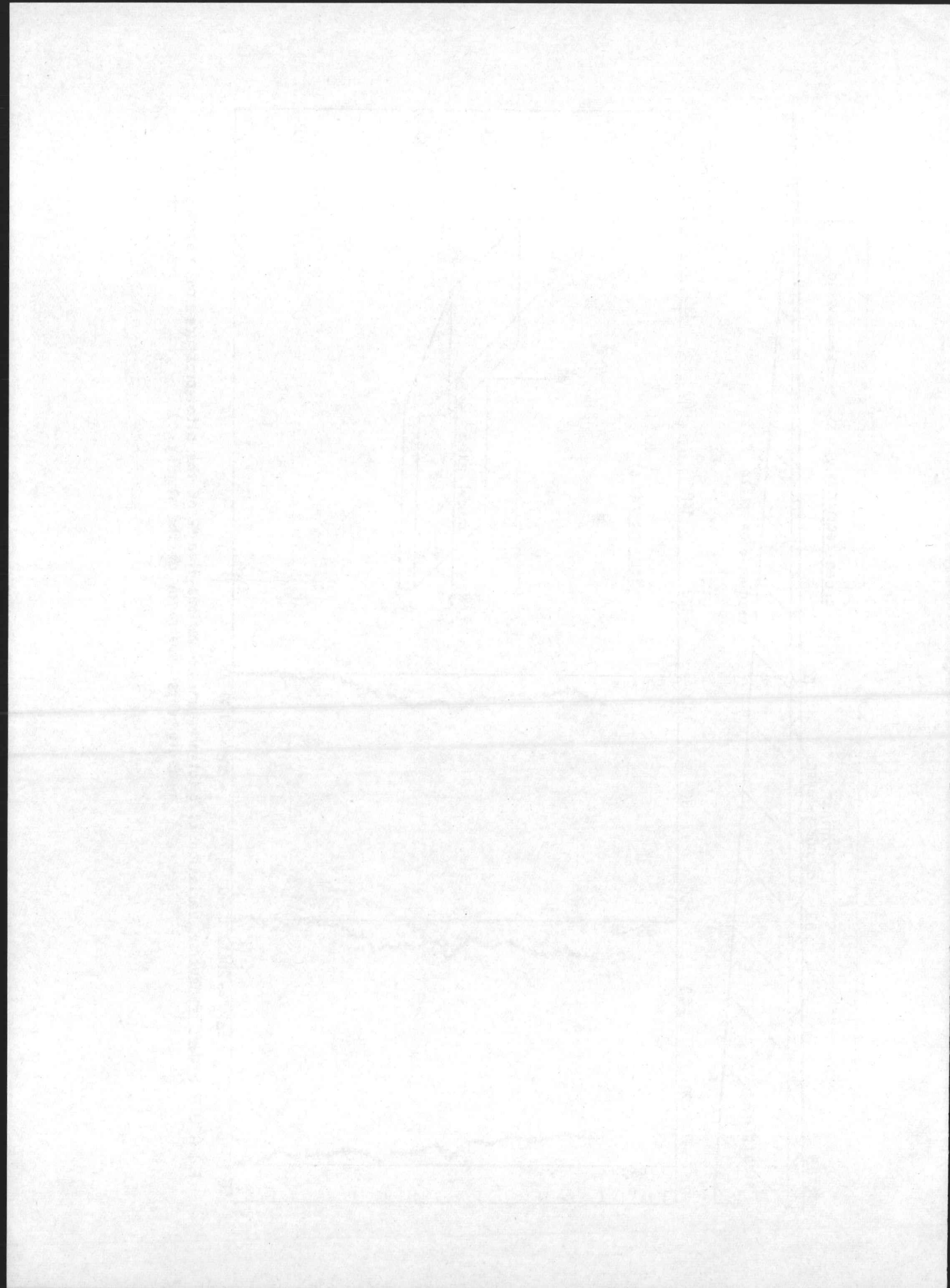


FIGURE 6.b - transverse variation of pitot-pressure at various x , in % of the pitot-pressure on model-axis. measurements upstream of the step ($x < 0$)



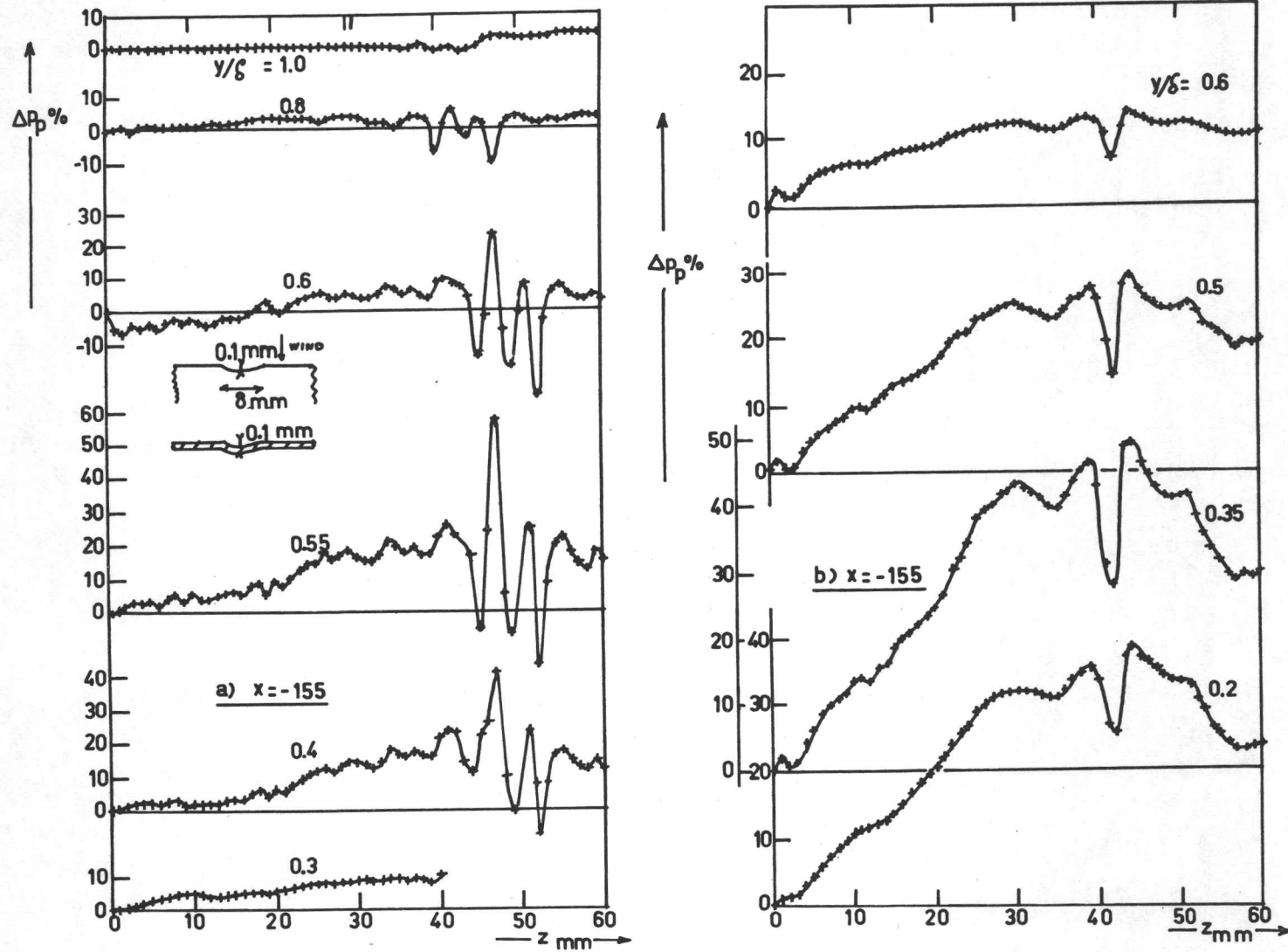
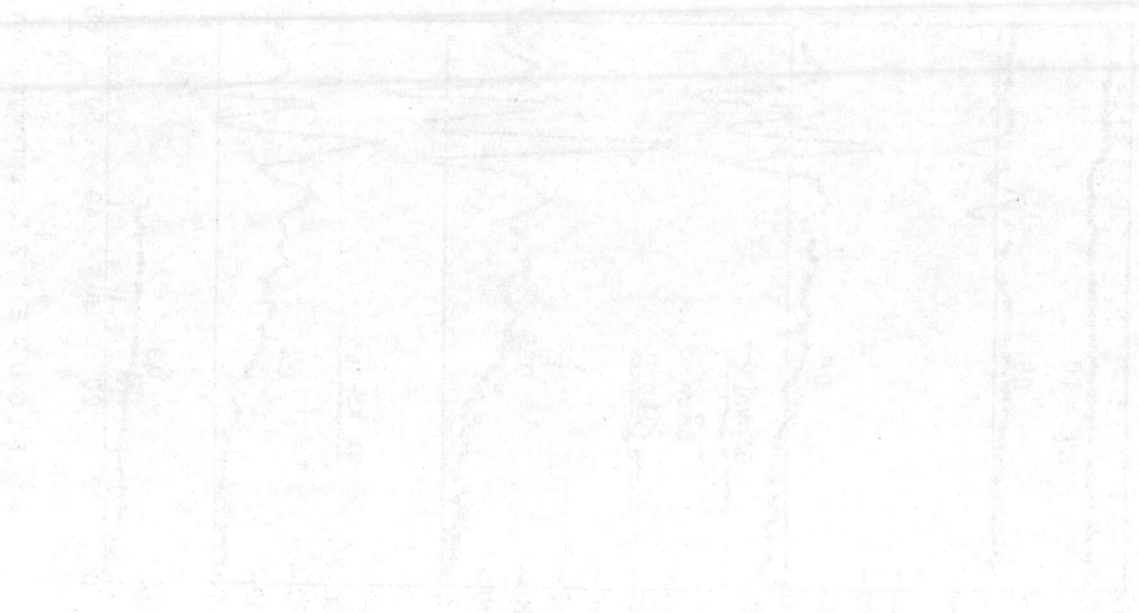


FIGURE 7 - surveys on model S-3 with accidental notches in the L.E.



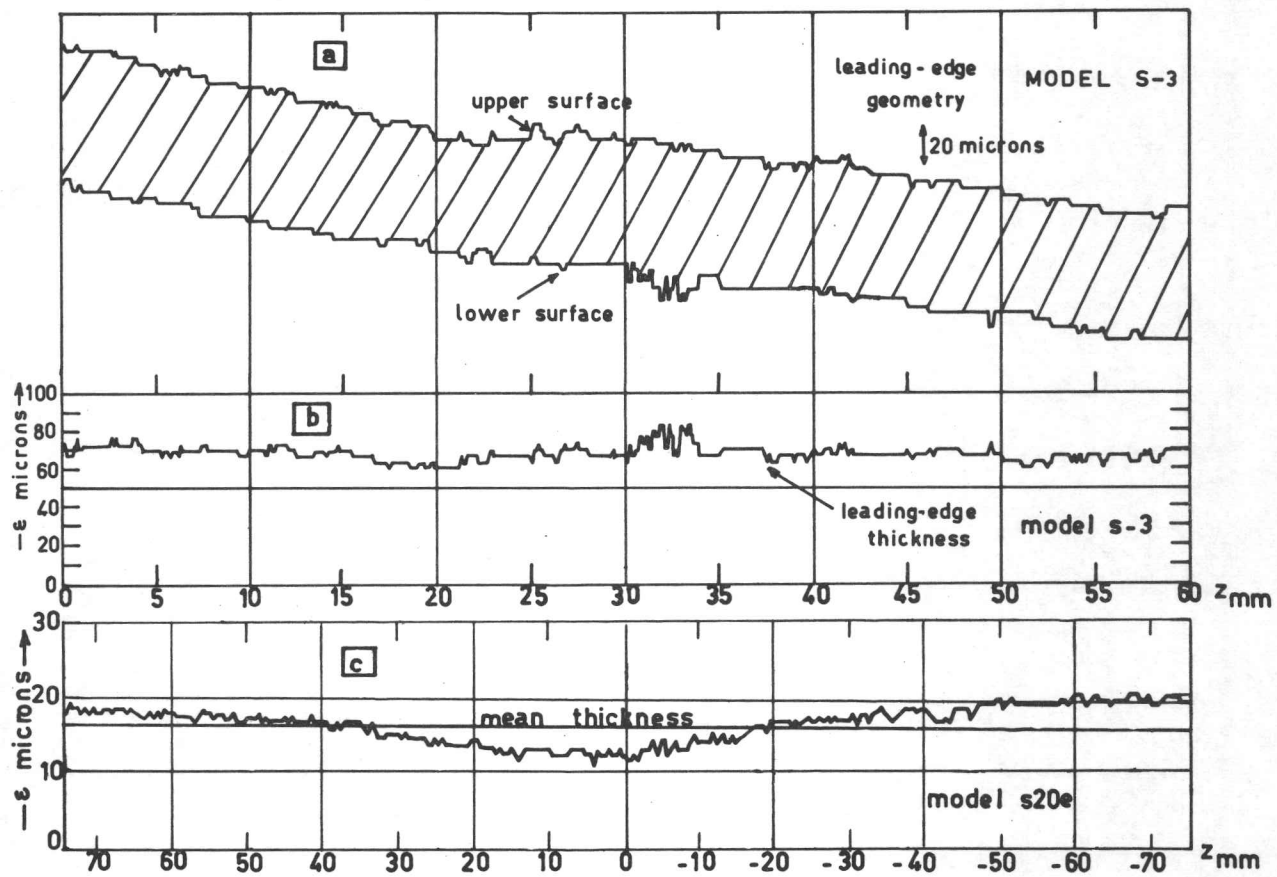
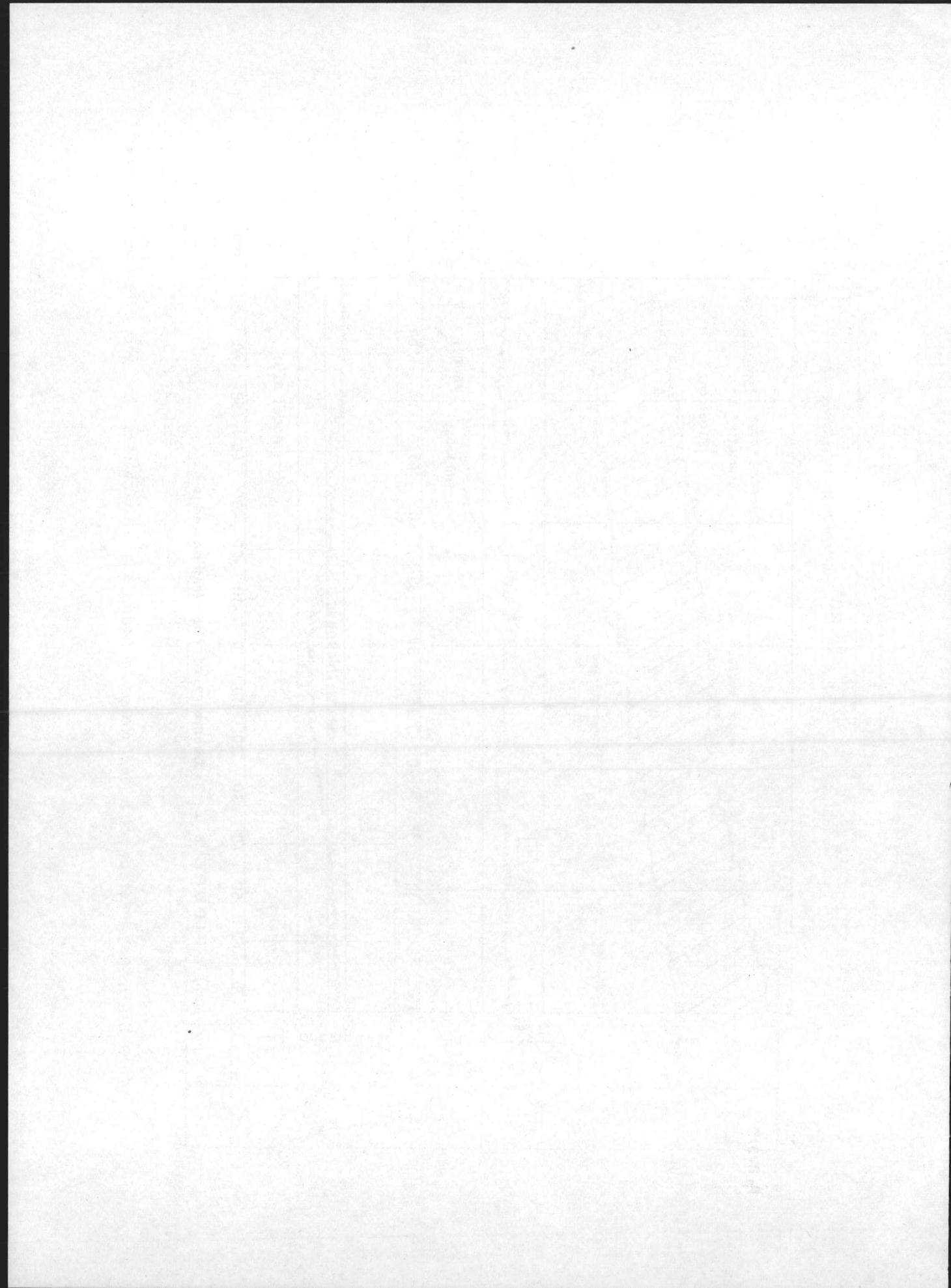


FIGURE 8 - Geometry of the leading-edge



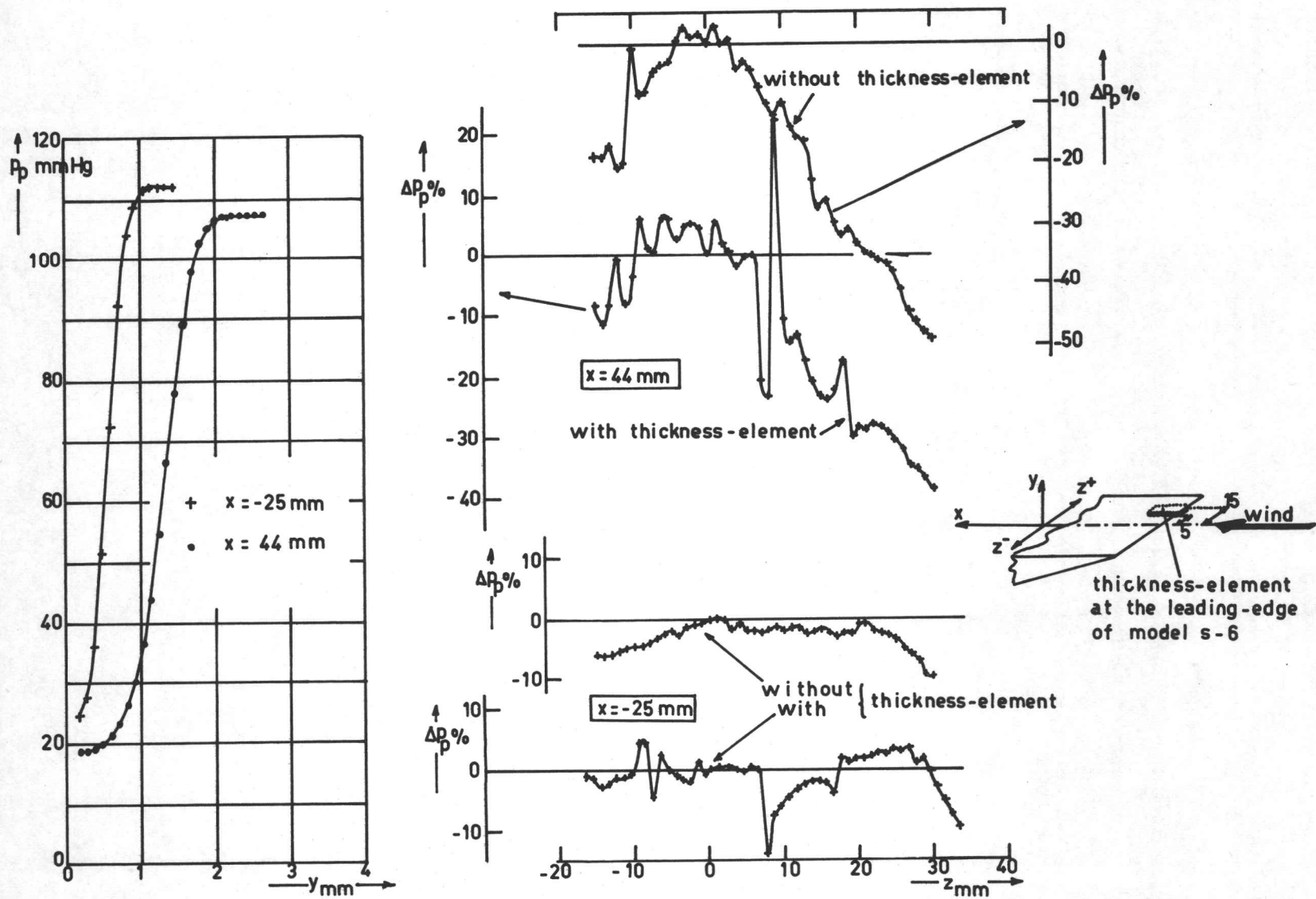


FIGURE 9 - Effect of a local change in leading-edge thickness on the flow perturbations

1. The first graph shows the relationship between the flow rate and the time taken for the water to pass through the pipe.



Graph 1: Flow rate vs. time

2. The second graph shows the relationship between the flow rate and the time taken for the water to pass through the pipe.



Graph 2: Flow rate vs. time

3. The third graph shows the relationship between the flow rate and the time taken for the water to pass through the pipe.



Graph 3: Flow rate vs. time

4. The fourth graph shows the relationship between the flow rate and the time taken for the water to pass through the pipe.



Graph 4: Flow rate vs. time

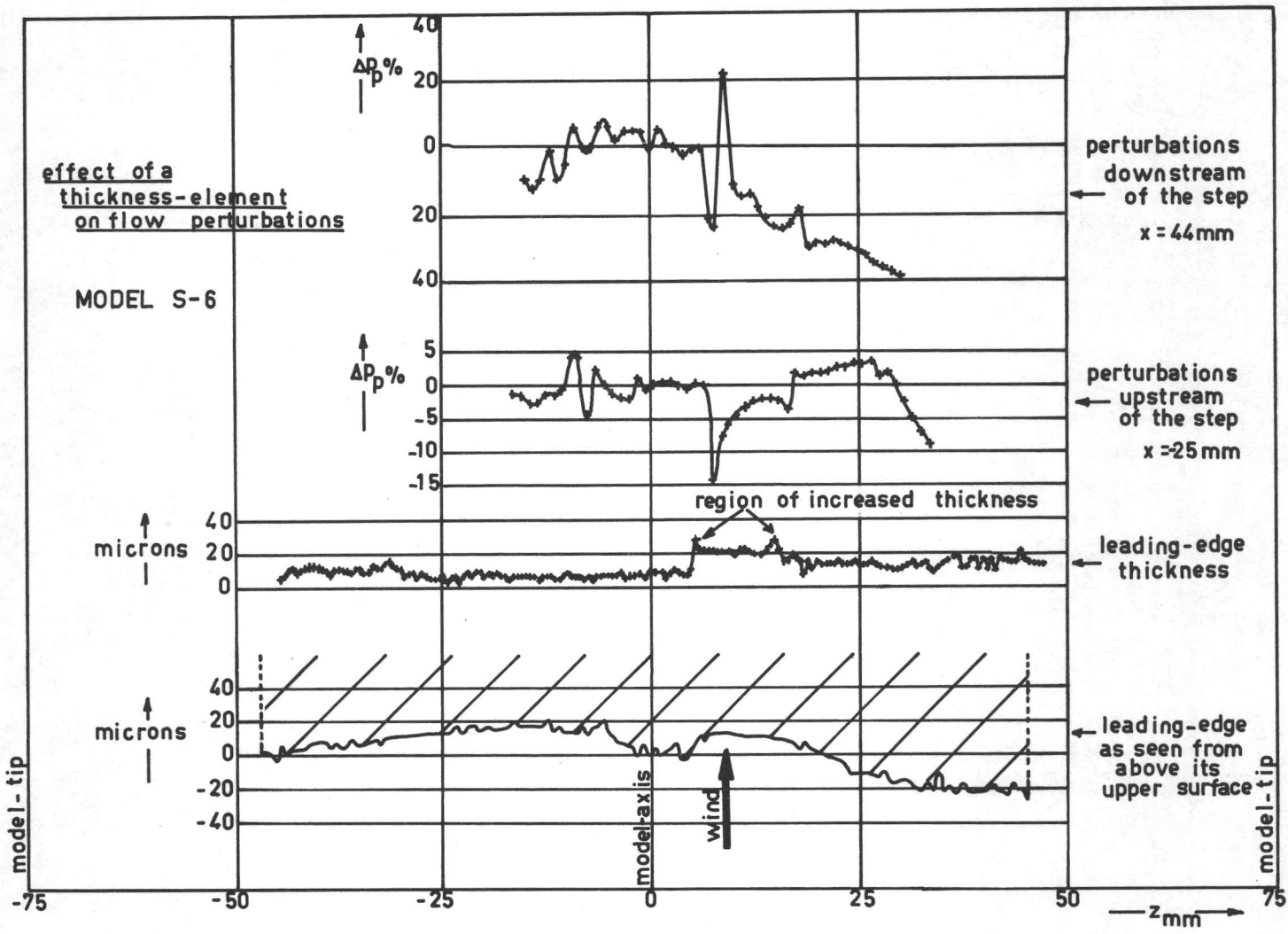
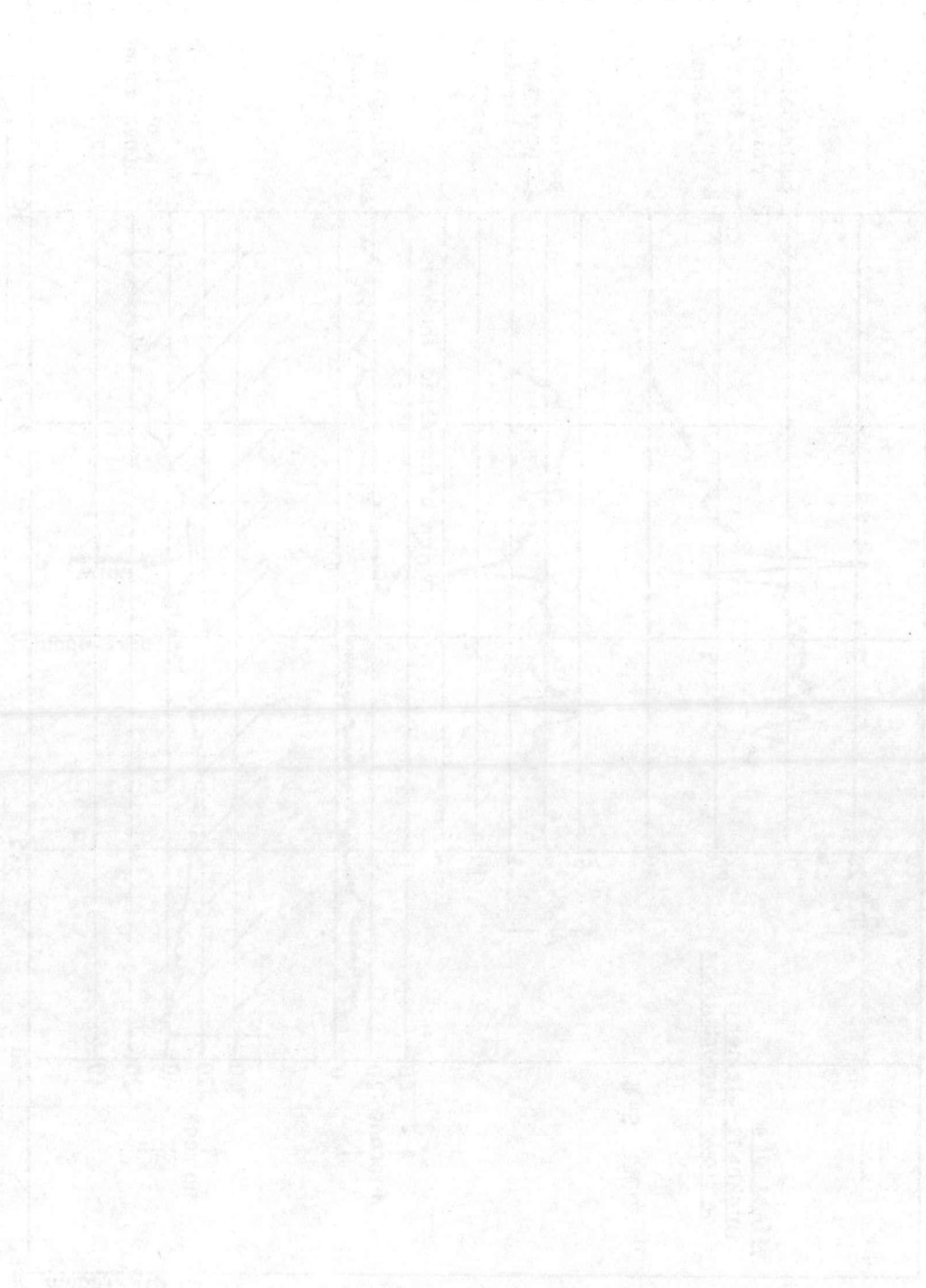


FIGURE 10 - Comparison between flow-perturbations and leading-edge geometry



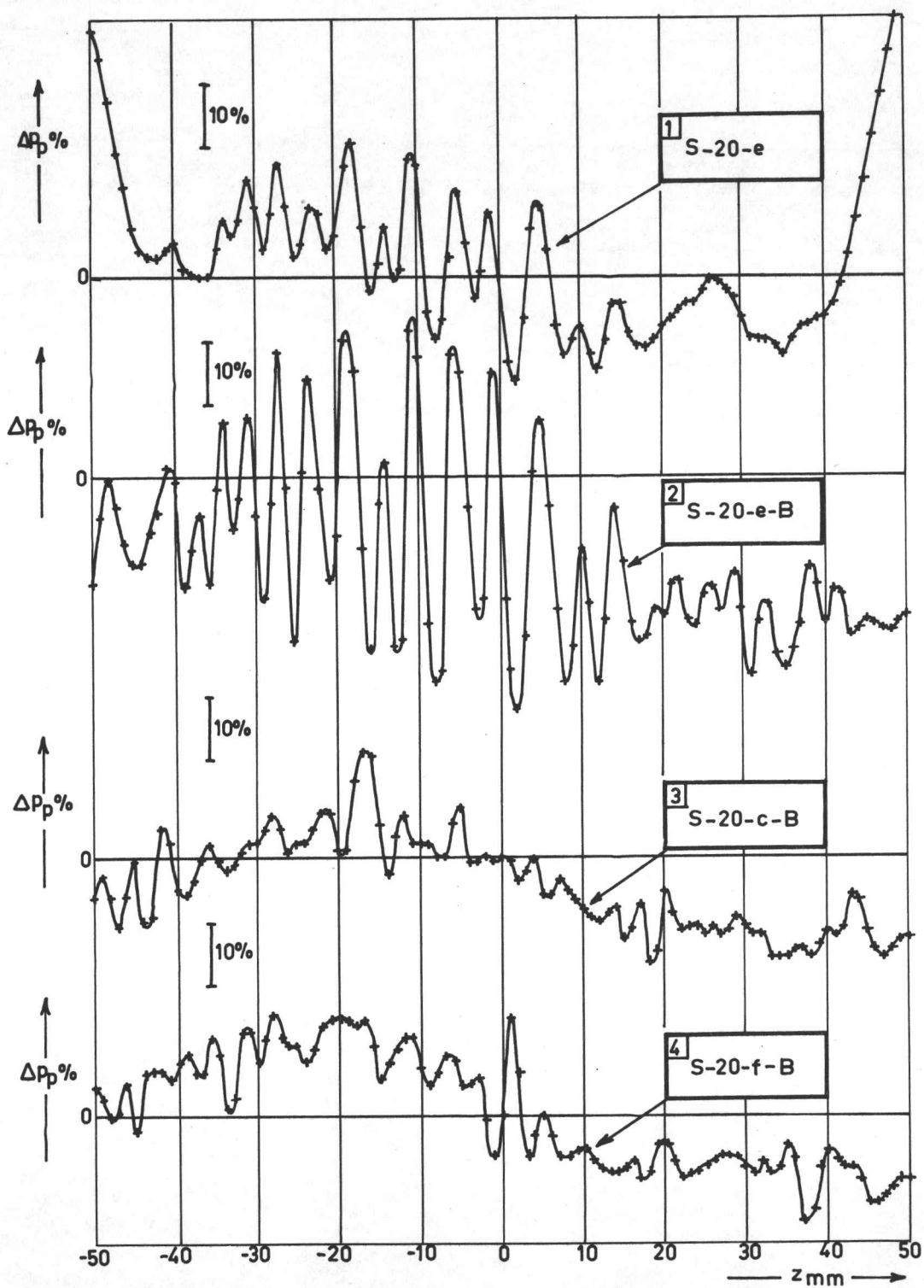
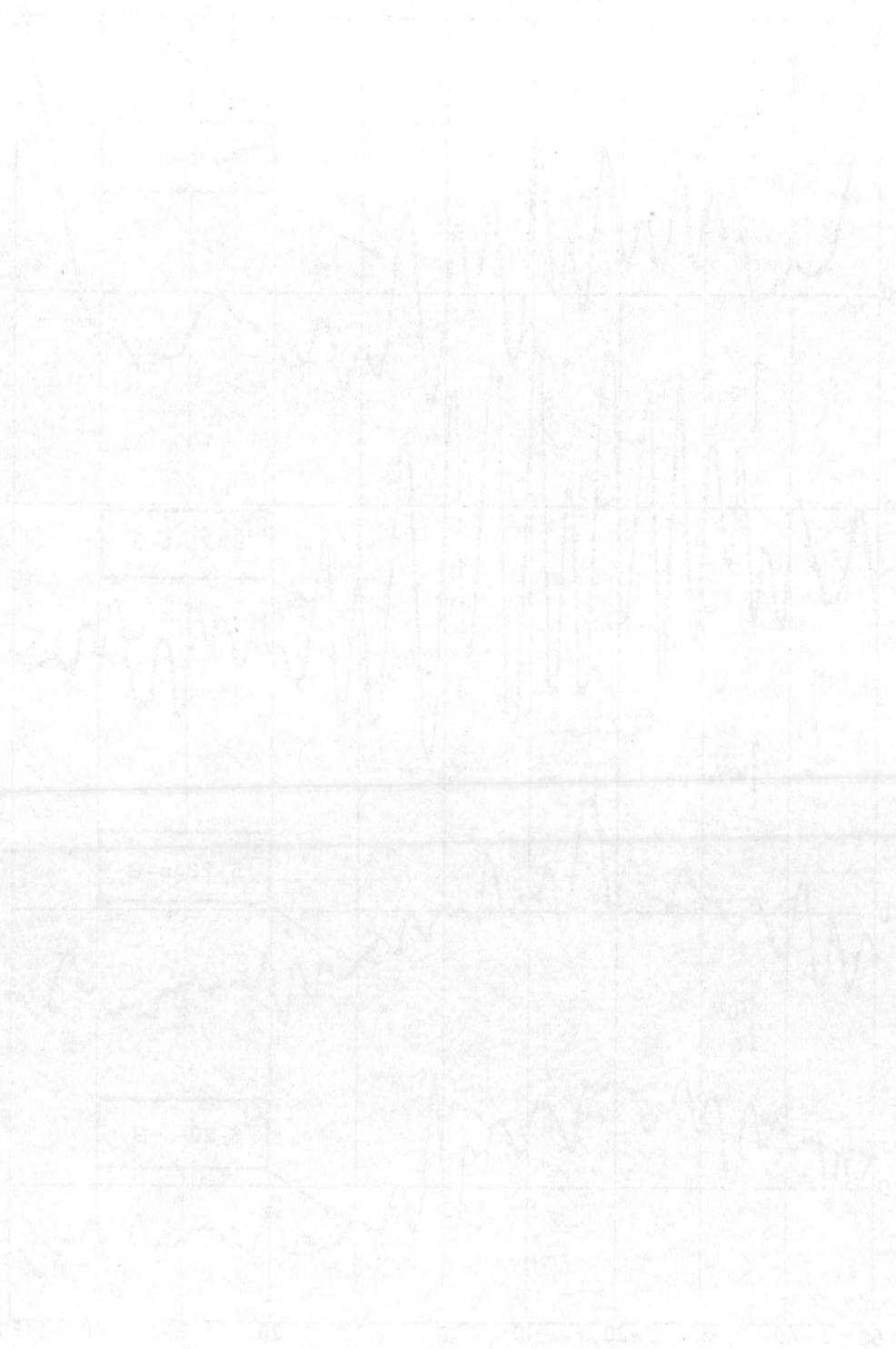
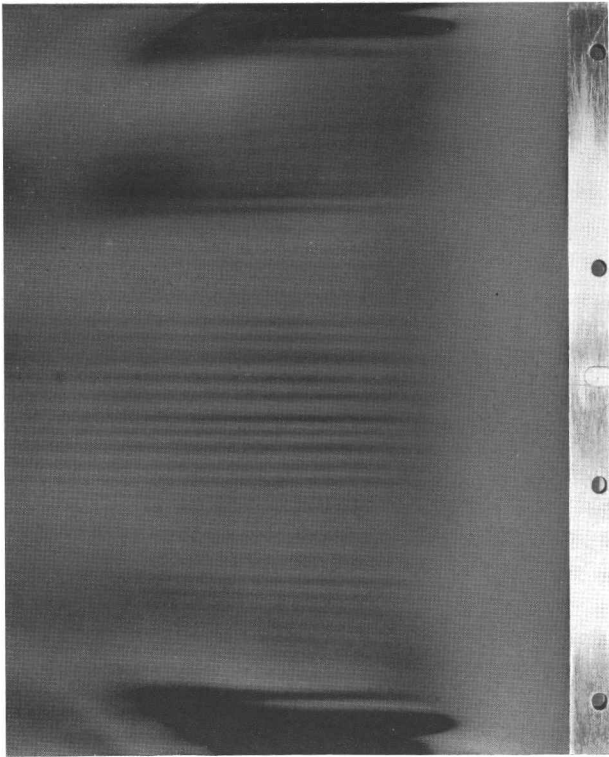


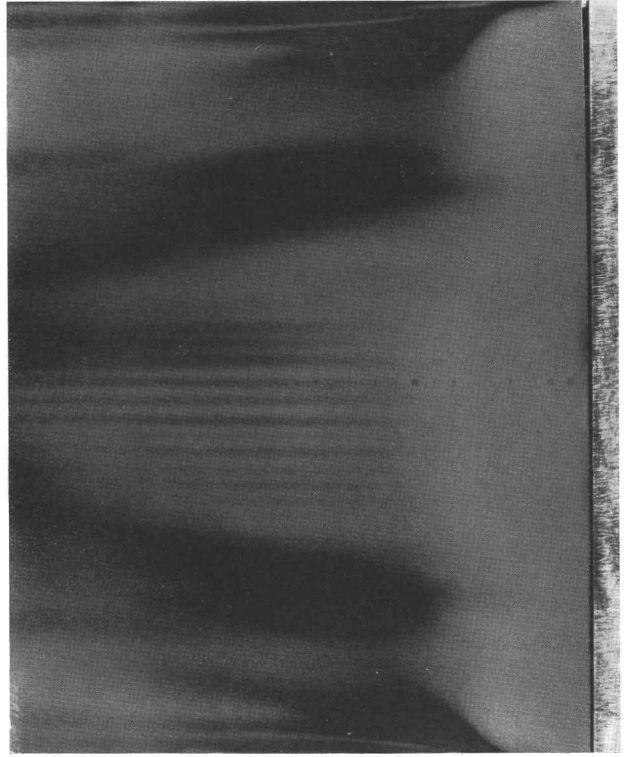
FIGURE 11 - Surveys made on models S - 20



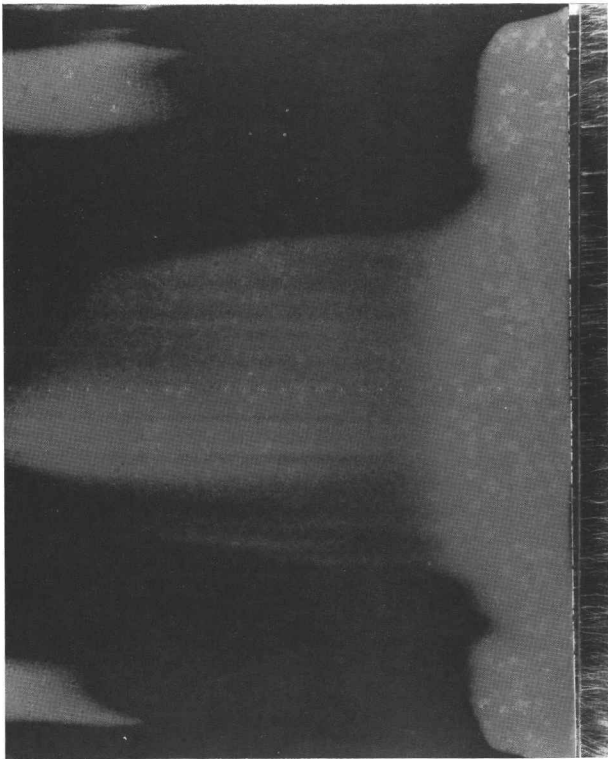
Handwritten text at the bottom of the page, possibly a signature or date, which is mostly illegible due to fading and blurring.



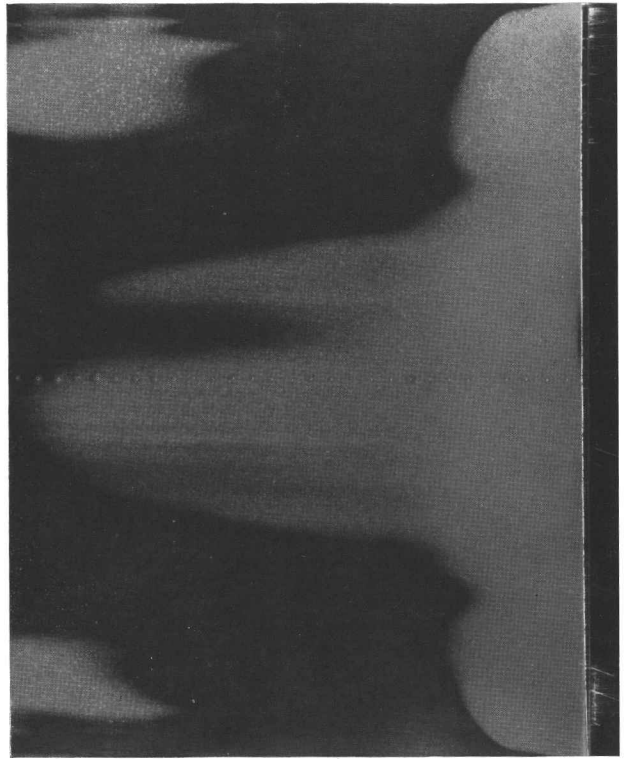
a) Model S-20-e-B



b) Model S-20-e

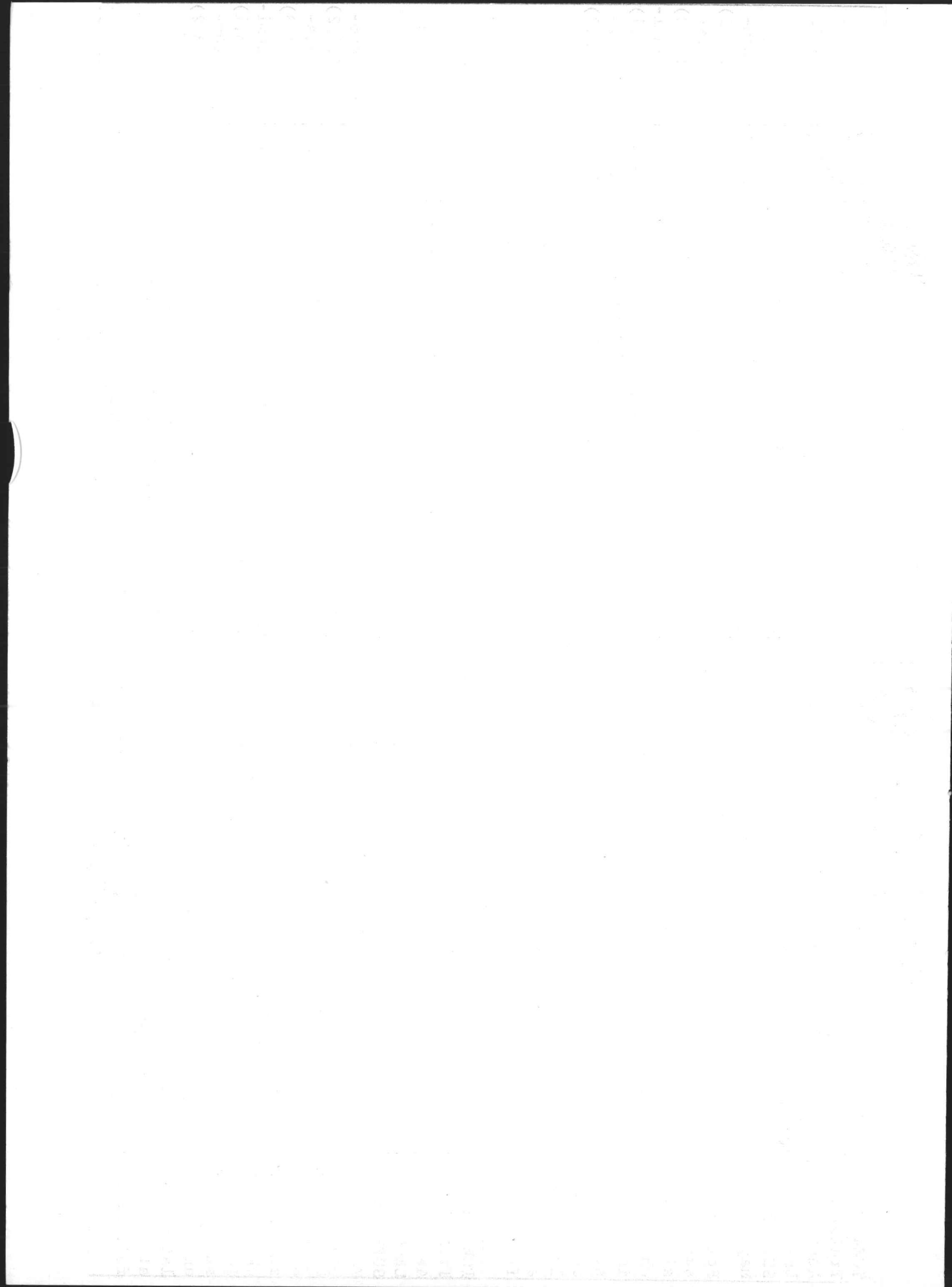


c) Model S-20-c



d) Model S-20-f

Figure 12. Sublimation technique



<p>TCEA TN 4 Training Center for Experimental Aerodynamics LEADING EDGE EFFECT ON SEPARATED SUPERSONIC FLOWS May 1961 Jean J. Ginoux</p> <p>Following earlier tests in the TCEA supersonic tunnel S-1, on a two-dimensional backward-facing step model in which span-wise perturbations were found in the reattachment region, further studies have been made using the same and other similar models. In these later studies, the same three-dimensional perturbations were detected into the full thickness of the boundary-layer,</p> <p style="text-align: right;">(over)</p>	<p>I. GINOUX, Jean J. II. TCEA TN 4.</p> <ol style="list-style-type: none"> 1. Flow, compressible (1.1.2) 2. Flow, viscous (1.1.3) 3. Flow, laminar (1.1.3.1) 4. Flow, turbulent (1.1.3.2) 	<p>TCEA TN 4 Centre de Formation en Aérodynamique Expérimentale INFLUENCE DU BORD D'ATTAQUE SUR LE COMPORTEMENT D'ECOULEMENTS SUPERSONIQUES DECOLLES Mai 1961 Jean J. Ginoux</p> <p>Une suite a été donnée à une étude expérimentale antérieure effectuée à la soufflerie supersonique S-1 du CFAE sur des modèles bidimensionnels constitués par des décrochements de paroi en forme de marche, au cours de laquelle des perturbations tridimensionnelles avaient été enregistrées dans la zone de recollement de la couche limite.</p> <p style="text-align: right;">(voir verso)</p>	<p>I. GINOUX, Jean J. II. TCEA TN 4.</p> <ol style="list-style-type: none"> 1. Ecoulement, compressible (1.1.2) 2. Ecoulement, visqueux (1.1.3) 3. Ecoulement, laminaire (1.1.3.1) 4. Ecoulement, turbulent (1.1.3.2)
<p>TCEA TN 4 Training Center for Experimental Aerodynamics LEADING EDGE EFFECT ON SEPARATED SUPERSONIC FLOWS May 1961 Jean J. Ginoux</p> <p>Following earlier tests in the TCEA supersonic tunnel S-1, on a two-dimensional backward-facing step model in which span-wise perturbations were found in the reattachment region, further studies have been made using the same and other similar models. In these later studies, the same three-dimensional perturbations were detected into the full thickness of the boundary-layer,</p> <p style="text-align: right;">(over)</p>	<p>I. GINOUX, Jean J. II. TCEA TN 4.</p> <ol style="list-style-type: none"> 1. Flow, compressible (1.1.2) 2. Flow, viscous (1.1.3) 3. Flow, laminar (1.1.3.1) 4. Flow, turbulent (1.1.3.2) 	<p>TCEA TN 4 Centre de Formation en Aérodynamique Expérimentale INFLUENCE DU BORD D'ATTAQUE SUR LE COMPORTEMENT D'ECOULEMENTS SUPERSONIQUES DECOLLES Mai 1961 Jean J. Ginoux</p> <p>Une suite a été donnée à une étude expérimentale antérieure effectuée à la soufflerie supersonique S-1 du CFAE sur des modèles bidimensionnels constitués par des décrochements de paroi en forme de marche, au cours de laquelle des perturbations tridimensionnelles avaient été enregistrées and la zone de recollement de la couche limite.</p> <p style="text-align: right;">(voir verso)</p>	<p>I. GINOUX, Jean J. II. TCEA TN 4.</p> <ol style="list-style-type: none"> 1. Ecoulement, compressible (1.1.2) 2. Ecoulement, visqueux (1.1.3) 3. Ecoulement, laminaire (1.1.3.1) 4. Ecoulement, turbulent (1.1.3.2)

On a montré qu'après recollement, ces perturbations s'éten-
daient dans toute l'épaisseur de la couche limite, tant dans
la région laminaire de l'écoulement que dans sa partie tur-
bulente, avec une amplitude maximum dans la zone de transition.

L'amélioration de la précision d'usinage du bord d'attaque
a permis de diminuer l'amplitude des perturbations (cette
dernière étant approximativement proportionnelle à la dimen-
sion des irrégularités du bord d'attaque) et cela sans que
la longueur d'onde des perturbations ne soit modifiée. Etant
donné qu'il est raisonnable de considérer ces irrégularités
comme réparties de manière aléatoire, il a été conclu que le
phénomène considéré représentait essentiellement une insta-
bilité de l'écoulement bidimensionnel, dont le déclenchement
était provoqué par des irrégularités extrêmement petites
dans le bord d'attaque.

Copies disponibles au CFAE, Rhode-St-Genèse, Belgique.

On a montré qu'après recollement, ces perturbations s'éten-
daient dans toute l'épaisseur de la couche limite, tant dans
la région laminaire de l'écoulement que dans sa partie tur-
bulente, avec une amplitude maximum dans la zone de transition.

L'amélioration de la précision d'usinage du bord d'attaque
a permis de diminuer l'amplitude des perturbations (cette
dernière étant approximativement proportionnelle à la dimen-
sion des irrégularités du bord d'attaque) et cela sans que
la longueur d'onde des perturbations ne soit modifiée. Etant
donné qu'il est raisonnable de considérer ces irrégularités
comme réparties de manière aléatoire, il a été conclu que le
phénomène considéré représentait essentiellement une insta-
bilité de l'écoulement bidimensionnel, dont le déclenchement
était provoqué par des irrégularités extrêmement petites
dans le bord d'attaque.

Copies disponibles au CFAE, Rhode-St-Genèse, Belgique.

after reattachment, both in turbulent and laminar regions
of the flow. Their amplitude was a maximum in the transi-
tion region.

In using a model with a much improved accuracy of manufac-
ture, notably at the leading-edge, it was found that the
amplitude of the perturbations was greatly reduced, roughly
in proportion to the size of the irregularities of manufac-
ture of the leading-edge itself. As it is unreasonable to
expect these to be anything other than random in character,
it is concluded that the phenomenon is essentially one of
instability in the two-dimensional flow, the main triggering
action arising, at least in the earlier tests, from small
irregularities in the leading-edge.

Copies available at TCEA, Rhode-St-Genèse, Belgium.

after reattachment, both in turbulent and laminar regions
of the flow. Their amplitude was a maximum in the transi-
tion region.

In using a model with a much improved accuracy of manufac-
ture, notably at the leading-edge, it was found that the
amplitude of the perturbations was greatly reduced, roughly
in proportion to the size of the irregularities of manufac-
ture of the leading-edge itself. As it is unreasonable to
expect these to be anything other than random in character,
it is concluded that the phenomenon is essentially one of
instability in the two-dimensional flow, the main triggering
action arising, at least in the earlier tests, from small
irregularities in the leading-edge.

Copies available at TCEA, Rhode-St-Genèse, Belgium.

<p>TCEA TN 4 Training Center for Experimental Aerodynamics LEADING EDGE EFFECT ON SEPARATED SUPERSONIC FLOWS May 1961 Jean J. Ginoux</p> <p>Following earlier tests in the TCEA supersonic tunnel S-1, on a two-dimensional backward-facing step model in which span-wise perturbations were found in the reattachment region, further studies have been made using the same and other similar models. In these later studies, the same three-dimensional perturbations were detected into the full thickness of the boundary-layer,</p> <p style="text-align: right;">(over)</p>	<p>I. GINOUX, Jean J. II. TCEA TN 4.</p> <ol style="list-style-type: none"> 1. Flow, compressible (1.1.2) 2. Flow, viscous (1.1.3) 3. Flow, laminar (1.1.3.1) 4. Flow, turbulent (1.1.3.2) 	<p>TCEA TN 4 Centre de Formation en Aérodynamique Expérimentale INFLUENCE DU BORD D'ATTAQUE SUR LE COMPORTEMENT D'ECOULEMENTS SUPERSONIQUES DECOLLES Mai 1961 Jean J. Ginoux</p> <p>Une suite a été donnée à une étude expérimentale antérieure effectuée à la soufflerie supersonique S-1 du CFAE sur des modèles bidimensionnels constitués par des décrochements de paroi en forme de marche, au cours de laquelle des perturbations tridimensionnelles avaient été enregistrées dans la zone de recollement de la couche limite.</p> <p style="text-align: right;">(voir verso)</p>	<p>I. GINOUX, Jean J. II. TCEA TN 4.</p> <ol style="list-style-type: none"> 1. Ecoulement, compressible (1.1.2) 2. Ecoulement, visqueux (1.1.3) 3. Ecoulement, laminaire (1.1.3.1) 4. Ecoulement, turbulent (1.1.3.2)
<p>TCEA TN 4 Training Center for Experimental Aerodynamics LEADING EDGE EFFECT ON SEPARATED SUPERSONIC FLOWS May 1961 Jean J. Ginoux</p> <p>Following earlier tests in the TCEA supersonic tunnel S-1, on a two-dimensional backward-facing step model in which span-wise perturbations were found in the reattachment region, further studies have been made using the same and other similar models. In these later studies, the same three-dimensional perturbations were detected into the full thickness of the boundary-layer,</p> <p style="text-align: right;">(over)</p>	<p>I. GINOUX, Jean J. II. TCEA TN 4.</p> <ol style="list-style-type: none"> 1. Flow, compressible (1.1.2) 2. Flow, viscous (1.1.3) 3. Flow, laminar (1.1.3.1) 4. Flow, turbulent (1.1.3.2) 	<p>TCEA TN 4 Centre de Formation en Aérodynamique Expérimentale INFLUENCE DU BORD D'ATTAQUE SUR LE COMPORTEMENT D'ECOULEMENTS SUPERSONIQUES DECOLLES Mai 1961 Jean J. Ginoux</p> <p>Une suite a été donnée à une étude expérimentale antérieure effectuée à la soufflerie supersonique S-1 du CFAE sur des modèles bidimensionnels constitués par des décrochements de paroi en forme de marche, au cours de laquelle des perturbations tridimensionnelles avaient été enregistrées and la zone de recollement de la couche limite.</p> <p style="text-align: right;">(voir verso)</p>	<p>I. GINOUX, Jean J. II. TCEA TN 4.</p> <ol style="list-style-type: none"> 1. Ecoulement, compressible (1.1.2) 2. Ecoulement, visqueux (1.1.3) 3. Ecoulement, laminaire (1.1.3.1) 4. Ecoulement, turbulent (1.1.3.2)

On a montré qu'après recollement, ces perturbations s'étendaient dans toute l'épaisseur de la couche limite, tant dans la région laminaire de l'écoulement que dans sa partie turbulente, avec une amplitude maximum dans la zone de transition.

L'amélioration de la précision d'usinage du bord d'attaque a permis de diminuer l'amplitude des perturbations (cette dernière étant approximativement proportionnelle à la dimension des irrégularités du bord d'attaque) et cela sans que la longueur d'onde des perturbations ne soit modifiée. Etant donné qu'il est raisonnable de considérer ces irrégularités comme réparties de manière aléatoire, il a été conclu que le phénomène considéré représentait essentiellement une instabilité de l'écoulement bidimensionnel, dont le déclenchement était provoqué par des irrégularités extrêmement petites dans le bord d'attaque.

Copies disponibles au CFAE, Rhode-St-Genèse, Belgique.

On a montré qu'après recollement, ces perturbations s'étendaient dans toute l'épaisseur de la couche limite, tant dans la région laminaire de l'écoulement que dans sa partie turbulente, avec une amplitude maximum dans la zone de transition.

L'amélioration de la précision d'usinage du bord d'attaque a permis de diminuer l'amplitude des perturbations (cette dernière étant approximativement proportionnelle à la dimension des irrégularités du bord d'attaque) et cela sans que la longueur d'onde des perturbations ne soit modifiée. Etant donné qu'il est raisonnable de considérer ces irrégularités comme réparties de manière aléatoire, il a été conclu que le phénomène considéré représentait essentiellement une instabilité de l'écoulement bidimensionnel, dont le déclenchement était provoqué par des irrégularités extrêmement petites dans le bord d'attaque.

Copies disponibles au CFAE, Rhode-St-Genèse, Belgique.

after reattachment, both in turbulent and laminar regions of the flow. Their amplitude was a maximum in the transition region.

In using a model with a much improved accuracy of manufacture, notably at the leading-edge, it was found that the amplitude of the perturbations was greatly reduced, roughly in proportion to the size of the irregularities of manufacture of the leading-edge itself. As it is unreasonable to expect these to be anything other than random in character, it is concluded that the phenomenon is essentially one of instability in the two-dimensional flow, the main triggering action arising, at least in the earlier tests, from small irregularities in the leading-edge.

Copies available at TCEA, Rhode-St-Genèse, Belgium.

after reattachment, both in turbulent and laminar regions of the flow. Their amplitude was a maximum in the transition region.

In using a model with a much improved accuracy of manufacture, notably at the leading-edge, it was found that the amplitude of the perturbations was greatly reduced, roughly in proportion to the size of the irregularities of manufacture of the leading-edge itself. As it is unreasonable to expect these to be anything other than random in character, it is concluded that the phenomenon is essentially one of instability in the two-dimensional flow, the main triggering action arising, at least in the earlier tests, from small irregularities in the leading-edge.

Copies available at TCEA, Rhode-St-Genèse, Belgium.